JOURNAL OF MORPHOLOGY 251:256–275 (2002)

Muscular Anatomy of the Millipede *Phyllogonostreptus nigrolabiatus* (Diplopoda: Spirostreptida) and Its Bearing on the Millipede "Thorax"

Heather M. Wilson*

Department of Entomology, University of Maryland, College Park, Maryland 20742
Published online xx Month 2001

ABSTRACT The muscular anatomy of the millipede *Phyllogonostreptus nigrolabiatus* (Newport, 1844) (Diplopoda; Spirostreptida; Harpagophoridae) is comprehensively surveyed. The musculature of the first three postcollum pleurotergites, the "thorax," and their associated appendages was found to be more complex than that of the postthoracic rings. It is hypothesized that the musculature of the postthoracic segments is derived relative to that of the thoracic segments, which retain primitively free sternites and are not diplosegments. This hypothesis is discussed relative to previous hypotheses positing that the anteriormost three leg-bearing rings in millipedes are diplosegments. The musculature of spirostreptid gonopods is described in detail for the first time. Comparison of the cephalic musculature is made with previously described musculature in Julida showing that, while many aspects of the musculature are conserved, there exist interordinal differences, documenting the potential utility of comparative anatomical studies for resolving millipede phylogeny. J. Morphol. 251:256–275, 2002.

KEY WORDS: Arthropoda; Harpagophoridae; morphology; musculature; Myriapoda; thorax

The interordinal relationships within Diplopoda are far from clear. In the only published cladistic analysis of millipede phylogeny at the interordinal level using external morphological characters, Enghoff (1984) was unable to resolve a trichotomy between Nematophora (Stemmiulida + Callipodida + Chordeumatida), Merocheta (Polydesmida) and Juliformia. Although Enghoff et al. (1993) subsequently joined Merocheta and Juliformia as sister groups, based on the possession of trunk segments composed of complete rings, progress in resolving diplopod relationships using morphology has been limited by the lack of discovery of new characters with phylogenetic utility. Thus far, phylogenetic analysis of gene sequences has not resolved relationships between millipede orders. Regier and Shultz (In press) conducted a phylogenetic analysis of Myriapoda using two nuclear protein-encoding genes, elongation factor-1α and RNA polymerase II. Although they were able to recover all the represented myriapod classes, they were not able to convincingly resolve relationships among the millipede orders.

Muscular anatomy is an obvious source of information for use in phylogenetic analysis. This approach has already shown its efficacy in studies of chelicerate skeletomuscular anatomy by Shultz (1993, 1999, 2000). Unfortunately, the existing literature on millipede skeletomuscular anatomy was developed haphazardly and before the advent of parsimony and matrix-based analytical methods, making assembly of a complete taxon-by-character matrix from the literature nearly impossible. For example, while Manton produced numerous detailed works on millipede musculature (1954, 1956, 1958, 1961), she named muscles for their inferred function or general position in the body and ignored many muscles that she did not regard as germane to her functional arguments, such as those associated with the viscera, genitalia, and nonmandibular cephalic appendages. Thus, in order to construct a matrix that contains empirically robust hypotheses of homology, a comprehensive restudy of the muscular anatomy of representatives from each of the millipede orders is warranted. The present study is the first in a planned series to exhaustively survey the muscular anatomy of representatives from all of the millipede orders with two main long-term objectives: 1) to develop an empirically robust system of muscular homology using the criteria of similar origin, insertion, and position relative to other muscles; and 2) to generate a matrix of morphological characters for phylogenetic analysis comparable in completeness to those routinely generated for molecular sequence data.

Contract grant sponsor: National Science Foundation; Contract grant number: DEB-0075605.*

*Correspondence to: Heather M. Wilson, Department of Entomology, 4112 Plant Sciences Building, University of Maryland, College Park, MD 20742. E-mail: wilsonhm@wam.umd.edu

DOI 10.1002/jmor.1087

TABLE 1. Exhaustive list of skeletal muscles of the spirostreptid millipede Phyllogonostreptus nigrolabiatus*

No.	Name	Description
Cephalic muscles		
a1	Median septum antennal m. = abductor antennae (S), levator antennae (M)	Arises on posteroproximal margin of first antennomere; passes dorsomedially; inserts on the ventral margin of the median septum posterior to *p3* (Fig. 3A–C).
a2	Medial antennal m. = levator articuli primi antennae (S)	Arises on proximal margin of first antennomere medially; passes ventromedially lateral to *a3;* inserts dorsally on posterior process of tentorium lateral to *a3* (Fig. 3A–C).
a3	Lateral antennal m. = depressor articuli primi antennae (S)	Arises on proximal margin of first antennomere laterally; passes ventromedially lateral to *a4;* inserts dorsally on posterior process of tentorium posterior to *a4* (Fig. 3C).
a4	Anterior antennal m. = adductor articuli primi antennae (S)	Arises on anteroproximal margin of first antennomere; passes ventromedially medial to *a3;* inserts dorsally on posterior process of tentorium anterior to *a3* (Fig. 3A–C).
e1	Anterior epipharyngeal m. = medianus palati (S)	Arises on lateral keel of epipharynx; passes dorsally; inserts on clypeus anteromedial to *e4* (Figs. 1A, 2A, 3A).
e2	Posterior epipharyngeal m. = m. subrectus palatinae (S)	Arises on lateral keel of epipharynx anterior to the pharynx; passes dorsally; inserts on clypeus posterior to *t1* (Figs. 1A, 2A, 3A).
e3	Posterolateral epipharyngeal m. = m. laminae palatinae (S)	Arises on epipharyngeal bar; passes posterodorsally; inserts on clypeus lateral to *e2* (Figs. 1A, 2A, 3A–B).
e4	Anterolateral epipharyngeal m.	Arises on epipharyngeal bar; passes dorsally along medial margin of *t1;* inserts on clypeus posterolateral to *e1* (Figs. 1A, 3B–C).
g1	Lamellae linguales m. = depressor tentorii a stipite interno (S)	Arises on posteromedial corner of lingual lobe of gnathochilarium; passes posterodorsally; inserts anteroventrally on lateral edge of hypopharyngeal lateral sclerite (Figs. 1B, 2D, 3A–B).
g2	Anterior gnathochilarial stipes m. = depressor tentorii a stipite externo (S)	Arises on medial edge of gnathochilarial stipes near junction of lamellae linguales with mentum; passes posterodorsally; inserts anteroventrally on lateral edge of hypopharyngeal lateral sclerite (Figs. 1B, 2D, 3A–C).
g3	Lateral mentum m. = depressor tentorii ab inframaxillari (S)	Arises on gnathochilarial mentum lateral to *g4* + *g5;* passes anterodorsally; inserts on lateral edge of hypopharyngeal lateral sclerite (Figs. 1B, 2D, 3A–B).
g4	Anteromedial mentum m. = spathularis (S)	Arises on gnathochilarial mentum medial to *g3* and anterior to *g5;* passes anterodorsally; inserts on midline at base of hypopharynx (Figs. 1B, 2D, 3A).
g5	Posteromedial mentum m.	Arises medial to *g3* and posterior to *g4* on gnathochilarial mentum; passes anterodorsally; inserts on midline at top of hypopharyngeal furrow (Figs. 1B, 2D, 3A).
g6	Posterolateral gnathochilarial stipes m. = levator stipitis (S)	Arises on lateral edge of gnathochilarial stipes posteriorly; passes posterodorsally; inserts on ventromedial corner of postoccipital flange lateral to *p6* (Figs. 1B, 3A–C).
g7	Posteromedial gnathochilarial stipes m. = depressor stipitis (S)	Arises on posteromedial corner of gnathochilarial stipes; passes dorsally medial to *g6;* inserts on ventral surface of transverse mandibular tendon lateral to *g8* (Figs. 1B, 3A–C).
g8	Medial intermentum m. = infrabasilaris (S)	Arises on intermentum of gnathochilarium medial to *g9;* passes anterodorsally; inserts on transverse mandibular tendon posteroventrally medial to *g7* (Figs. 1B, 3A).
g9	Lateral intermentum m. = infrabasilaris a pseudoccipite (S)	Arises on intermentum of gnathochilarium lateral to *g8;* passes posterodorsally; inserts on ventromedial corner of postoccipital flange (Figs. 1B, 3A–B).
m1	Gnathal lobe sclerite m. = adductor mandibulae (M), adductor praemandibulae (S)	Arises on gnathal lobe sclerite; passes posterodorsally; inserts on median septum and posterodorsal surface of cranium posterior to eyes (Figs. 1A, 2B, 3A–B).
m2	Dorsal mandibular stipes m. = levator mandibulae (M), abductor mandibulae (S)	Arises on anteromedial edge of mandibular stipes; passes posteriorly ventral to *m1;* inserts on postoccipital flange lateral to *t3* (Figs. 2B, 3C).
m3	Proximal gnathal lobe m.	Arises on proximal margin of gnathal lobe; passes posteriorly dorsal to *m6–m8* and ventral to lateral bar of tentorium; inserts on dorsal surface of gnathal lobe sclerite (Fig. 2B).
m4	Anterior mandibular cardo m. = dilator tentorii minor (M, S)	Arises on medial edge of tentorium with *m5;* passes ventrolaterally; inserts on dorsolateral wall of mandibular cardo anteriorly (Figs. 2C, 3C).
m5	Posterior mandibular stipes m. = dilator tentorii major (M, S)	Arises on medial edge of tentorium with *m4;* passes ventrolaterally; inserts on dorsolateral wall of mandibular stipes posteriorly (Figs. 2C, 3C).
m6	Ventral mandibular stipes m. = adductor mandibulae from stipes (M), adductor mandibulae pars stipitis (S)	Arises on middle branch of transverse mandibular tendon; passes laterally/ventrolaterally ventral to *m4–m7;* inserts on inner surface mandibular stipes not occupied by *m5* or *m7* (Fig. 2C, D).
m7	Anterior mandibular stipes m. = intrinsic levator from gnathal lobe (M), levator praemandibulae (S)	Paired. Arises from anterior branch of transverse mandibular tendon along with *m8;* passes laterally; inserts on inner lateral wall of mandibular stipes anteriorly (Fig. 2C, D).

TABLE 1. (Continued)

No.	Name	Description
Cephalic muscles (continued)		
m8	Gnathal lobe m. = adductor mandibulae from gnathal lobe (M)	Arises from anterior branch of transverse mandibular tendon along with *m7;* passes anterodorsally into mandibular gnathal lobe; inserts on inside dorsal surface of gnathal lobe (Fig. 2C).
m9	Posterior mandibular cardo m. = adductor mandibulae from cardo (M), adductor mandibulae pars cardinis (S)	Arises from posterior branch of transverse mandibular tendon; passes posterolaterally; inserts on posterodorsal corner of mandibular cardo posterior to *m4* (Fig. 2C, D).
p1	Precerebral pharyngeal dilator m. = dilator pharingis anticus a fronte (S)	Arises from anterior of pharynx dorsally; passes dorsally; inserts on cranium medial to *t2* (Figs. 1A, 2A, 3A).
p2	Intercerebral pharyngeal dilator m. = dilator pharingis posticus a fronte (S)	Arises from pharynx dorsally posterior to *p1;* passes dorsally through the cerebral perforation; inserts on the cranium posterior to *p1* (Figs. 1A, 2A, 3A).
p3	Median septum pharyngeal dilator m. = dorsal pharyngeal dilator (M), dilator pharingis a crista verticis	Arises on dorsal surface of pharynx; passes dorsally; inserts at anterior of median septum (Figs. 2A, 3A).
p4	Dorsal postoccipital flange pharyngeal dilator m. = postero-dorsal pharyngeal dilator (M), dilator pharingis a pseudoccipite (S)	Arises from the ventral margin of the dorsal portion of the postoccipital flange; passes ventrally; inserts on the pharynx dorsally posterior to *p3* (Figs. 2A, 3A).
p5	Tentorial pharyngeal dilator m. = dilator pharingis a tentorio (S)	Arises on medial surface of posterior process of tentorium; passes medially; inserts on pharynx laterally posterior to *p1* (Fig. 2A, B).
p6a,b	Transverse mandibular tendon pharyngeal dilator m. = dilator pharingis posticus + anticus a tendine subpharingeo (S)	Divided into a larger posterior muscle and a smaller anterior muscle. Arises on transverse mandibular tendon medial to *t4;* passes dorsally; inserts on the pharynx ventrally anterior to *p7* (Figs. 2C–D, 3A).
p7	Ventral postoccipital flange pharyngeal dilator m. = dilator pharingis inferior a pseudoccipite (S)	Arises on ventromedial corner of postoccipital flange medial to *g6;* passes anterodorsally mesial to *tt1;* inserts on pharynx ventrally posterior to *p6a* (Fig. 3A).
t1	Anterior tentorial m. = protractor tentorii (M, S)	Arises on lateral bar and anterior process of tentorium; passes anterodorsally; inserts on anterior of cranium (Figs. 1A, 2A, 3B–C).
t2	Dorsal tentorial m. = levator tentorii (M, S)	Arises on anterior process of tentorium; passes dorsally; inserts on cranium mesial to antennal socket and lateral to *p1* (Figs. 1A, 2A, 3A–B).
t3	Posterior tentorial m. = retractor tentorii (M, S)	Arises on posterior process of tentorium; passes posteriorly; inserts on postoccipital flange lateral to *tt1* and mesial to *m2* (Figs. 2A, 3B).
t4	Ventral tentorial m. = constrictor tentorii (S)	Arises on medial edge of tentorium; passes ventrally; inserts on transverse mandibular tendon lateral to *p6a, b* (Fig. 2C–D, 3B).
tt1	Posterior transverse mandibular tendon m. = retractor from transverse mandibular tendon (M), retractor tendinis subpharingei (S)	Arises on posterior of transverse mandibular tendon; passes posterodorsally; inserts on postoccipital flange medial to *t3* (Figs. 2C–D, 3A–B).
Collum muscles		
c1	postoccipital flange-t2 longitudinal m. = levator capitis superior (S)	Arises on postoccipital flange paramedially; passes posteriorly; inserts on anterior of t2 phragma paramedially (Fig. 5A).
c2	Postoccipital flange-t2 phragma oblique m. = depressor capitis anterior (S)	Arises on ventromedial corner of postoccipital flange laterally; passes posterodorsally; inserts on anterior of t2 phragma shallow to *c1* (Fig. 5A–C).
c3	Dorsal postoccipital flange oblique m.	Arises on medial edge of postoccipital flange dorsal to *c1;* passes posterodorsally between *c1* and *c3;* inserts on dorsal surface of t1 paramedially (Fig. 5A, B).
c4	Medial occipital flange oblique m. = retractor capitis (S)	Arises on medial edge of postoccipital flange dorsal to *c1* and shallow to *c2;* passes posterodorsally shallow to *c2;* inserts on dorsolateral surface of t1 (Fig. 5A, B).
c5	Postoccipital flange-t2 oblique m. = depressor capitis posterior (S)	Arises on ventromedial corner of postoccipital flange; passes posterodorsally; inserts on dorsolateral surface of t2 superficial to *pt3* (Fig. 5B, C).
c6	Gula-postoccipital flange m. = depressor basilaris anticus (S)	Arises on gula laterally; passes anterodorsally superficial to *va1h;* inserts on occipital flange laterally (Fig. 5D).

TABLE 1. (Continued)

No.	Name	Description
Collum muscles (continued)		
spt	Syncoxosternal-pleurotergal m. = depressor basilaris posticus (S)	Arises on gula laterally; passes dorsally deep to *vc* and shallow to *vh;* inserts on dorsolateral surface of collum anterior to *pt5* (Fig. 5C, D).
Trunk muscles		
pt1	Dorsal longitudinal pleurotergal m. = retractor dorsalis (M, S)	Arises dorsally on phragma of pleurotergite paramedially; passes posteriorly; inserts on phragma of following pleurotergite (Figs. 4, 5A, 6A–B, 8A–B).
pt2	Deep dorsal oblique pleurotergal m. = flexor internus dorsalis (M)	Arises dorsally on phragma of pleurotergite paramedially; passes anteroventrally deep to *pt3* and superficial to *pt1;* inserts on phragma of preceding pleurotergite (Figs. 4, 5B).
pt3	Shallow dorsal oblique pleurotergal m. = flexor externus dorsalis (M, S)	Arises dorsolaterally on phragma of pleurotergite; passes anterodorsally superficial to *pt2* and deep to *pt5;* inserts on dorsolateral wall of preceding pleurotergite (Figs. 4, 5B).
pt4	Deep lateral longitudinal pleurotergal m. = flexor inferus longus (M, S)	Arises ventrolaterally on phragma of pleurotergite; passes posteriorly deep to *pt4* and superficial to *va2;* inserts on phragma of following pleurotergite (Figs. 4, 5B–D, 6A–B, 8A–B).
pt5	Lateral oblique pleurotergal m. = involvens (M, S)	Arises from projection on phragma of pleurotergite laterally; passes anterodorsally superficial to *pt3* and dorsal to ozadene; inserts on dorsolateral wall of preceding pleurotergite (Figs. 4, 5A–D, 6A–B, 8A–B).
pt6	Shallow lateral longitudinal pleurotergal m. = retractor paratergalis (M, S)	Arises dorsolaterally on phragma of pleurotergite; passes posteriorly deep to *pt7* and superficial to *pt4;* inserts on phragma of following pleurotergite (Fig. 4).
pt7	Ventral oblique pleurotergal m. = flexor inferus brevis (M, S)	Arises ventrolaterally from the phragma of pleurotergite; passes anterolaterally superficial to *pt4;* inserts on phragma of preceding pleurotergite (Figs. 4, 5D).
pt8	Sternal oblique pleurotergal m. = flexor sternalis (M, S)	Arises ventrally from the phragma of pleurotergite paramedially anterior to the sternite; passes anterolaterally superficial to *pt7;* inserts on ventrolateral surface of preceding pleurotergite (Figs. 4, 5D, 6A–B).
Ventral apodeme muscles		
val$^{(1,2)}$	Longitudinal ventral apodeme-apodeme m. = retractor ventralis (M, S)	Arises laterally from anterior tracheal pouch of pair; passes posteriorly; inserts on first tracheal pouch of following pair. Some fibers of this muscle arise on posterior tracheal pouch of pair and insert on anterior tracheal pouch of following ring, and some fibers run from anterior to posterior tracheal pouch of a pair. In anterior trunk rings, *va1* splits into dorsal (*va*^{1}) and ventral (*va*^{2}) components (Figs. 4, 5A–C, 6A–B, 8A–B, 10B–F).
va2	Ventral apodeme-phragma m. = levator apophysis posticae (S)	Arises laterally from second tracheal pouch of pair; passes posterodorsally deep to *pt4;* inserts on anterior of phragma of following diplotergite (Figs. 4, 5A–C, 6A–B, 8A–B, 10B, C, F).
va3	Upper ventral apodeme-pleurotergal m.	Arises on the dorsal tip of the ventral apodeme; passes dorsally deep to *ist;* inserts on the dorsolateral surface of the pleurotergite anteriorly (Figs. 5A–C, 10A, C, E).
va4	Lower ventral apodeme-pleurotergal m.	Arises on the lateral edge of the ventral apodeme ventral to *va3;* passes ventrally anterior to *isp;* inserts on anteromedial corner of pleurotergite (Figs. 10A, C, F).
vg	Ventral apodeme 1-gula m.	Arises on the anterior face of ventral apodeme 1; passes anteroventrally; inserts on the lateral corner of the gula (Figs. 5B, 10A–B).
vh	Ventral apodme 1-cephalon m.	Arises on the anterior face of ventral apodeme 1 lateral to *va1g;* passes anteriorly; inserts on the occipital flange (Figs. 5C, 10A).
vc	Ventral apodeme 1-collum m.	Arises on the anterior face of ventral apodeme 1; passes anteriorly; inserts on the posterior margin of the anterior doublure of the collum laterally (Figs. 5C–D, 10A).
Anal muscles		
av1	Dorsal anal valve m.	Arises on the phragma and dorsolateral wall of the preanal ring; passes posteriorly; inserts on anterodorsal corner of anal valve (Fig. 8A, B).
av2	Ventral anal valve m.	Arises on the phragma and ventrolateral wall of the preanal ring; passes posteriorly; inserts on anteroventral corner of anal valve (Fig. 8A, B).
ad1	Anterior anal dilator m.	Arises on posterior surface of phragma of preanal ring; passes anterodorsally deep to *pt1;* inserts on posterior of rectum laterally anterior to *ad2* (Fig. 8B).
ad2	Posterior anal dilator m.	Arises on posterior surface of phragma of preanal ring; passes posteroventrally deep to *av1;* inserts on posterior of rectum laterally (Fig. 8A, B).
esl	Lateral eversible anal sac m.	Multiple muscles that arise on the phragma and pleurotergite of the preanal ring shallow to *esm;* pass posteriorly shallow to *esm;* insert on eversible anal sac in region of anal valve doublure (Fig. 8A, B).
esm	Medial eversible anal sac m.	Multiple muscles that arise on the phragma of the preanal ring; pass posteriorly deep to *esl;* insert on eversible anal sac antero medial to *esl* (Fig. 8A, B).
esl	Lateral eversible anal sac m.	Multiple muscles that arise on the phragma and pleurotergite of the preanal ring shallow to *esm;* pass posteriorly shallow to *esm;* insert on eversible anal sac in region of anal valve doublure (Fig. 8A, B).
esl	Lateral eversible anal sac m.	Multiple muscles that arise on the phragma and pleurotergite of the preanal ring shallow to *esm;* pass posteriorly shallow to *esm;* insert on eversible anal sac in region of anal valve doublure (Fig. 8A, B).

TABLE 1. (Continued)

Anal muscles (continued)		
esl	Lateral eversible anal sac m.	Multiple muscles that arise on the phragma and pleurotergite of the preanal ring shallow to *esm;* pass posteriorly shallow to *esm;* insert on eversible anal sac in region of anal valve doublure (Fig. 8A, B).
esm	Medial eversible anal sac m.	Multiple muscles that arise on the phragma of the preanal ring; pass posteriorly deep to *esl;* insert on eversible anal sac antero medial to *esl* (Fig. 8A, B).
Genital muscles		
pva♂	Penes-ventral apodeme m. (figured by Verhoeff 1926–1932, fig. 290) in (*Scaphiostreptus molleri*)	Arises on proximal edge of penes; passes dorsally anterior to intercalary sclerite and *sc2va;* inserts on posterior surface of ventral apodeme of t3 ventral to val^2 (Fig. 10D).
Intercalary sclerite muscles		
isp	Intercalary sclerite-pleurotergite m.	Arises on the dorsolateral edge of the intercalary sclerite; passes posterodorsally superficial to *va3;* inserts on the phragma of the following pleurotergite (Figs. 5B, D, 10B, D, F).
Extrinsic leg muscles		
ap	Appendicular protractor m.	Arises from proximolateral corner of coxa; passes anterodorsally superficial to *ar;* inserts on median bridge of ventral apodeme (Figs. 9, 10C, E).
ar	Appendicular retractor m.	Arises from tendon on proximomedial corner of coxa; passes anterodorsally deep to *ap;* inserts on median bridge of ventral apodeme (Figs. 9, 10F).
spt	Syncoxosternal-pleurotergal m.	Arises on dorsolateral corner of syncoxosternite; passes dorsally; inserts on pleurotergite (Figs. 5C–D, 10A, C).
sc2va ♂	Syncoxosternite2-ventral apodeme2 m.	Arises on dorsomedial corner of syncoxosternite 2; passes dorsally anterior to intercalary sclerite 2 and posterior to *pva;* inserts on posterior face of ventral apodeme 2 ventral to val^2 and medial to *pva* (Fig. 10D).
ova	Oblique coxa-ventral apodeme m.	Arises on anterior proximolateral edge of coxa (or coxal region of syncoxosternite); passes anterodorsally; inserts on medial edge of preceding ventral apodeme (Figs. 5B, 10A, C, E).
ova^c	Chiasmatic oblique coxa-ventral apodeme m.	Arises on anterior proximomedial edge of coxa (or coxal region of syncoxosternite); passes anterodorsally, crossing over the other muscle of the pair; inserts on medial edge of preceding ventral apodeme on opposite side of body medial to *ova* (Figs. 5A, 10A, C, E).
og	Chiasmatic oblique gula-ventral apodeme 1 m.	Arises on anterior edge of syncoxosternite 1 medial to ventral apodeme; passes anteriorly; crossing other muscle of the pair; inserts on posterolateral corner of gula (Figs. 5A, 10A–B).
Intrinsic leg muscles		
prfl	Prefemur levator m. = levator prefemoris (M)	Arises on dorsoproximal corner of prefemur; passes proximally deep to *prfd;* inserts proximally on coxa (Figs. 9, 10E).
prfd	Prefemur depressor m. = depressor prefemoris (M)	Arises on ventroproximal corner of prefemur; passes proximally superficial to *prfl;* inserts proximally on anterior and posterior faces of coxa (Figs. 9, 10E).
prfr	Prefemur retractor m.	Arises on posteroproximal margin of prefemur of leg 1; passes proximally superficial to *fed;* inserts on posterior face of syncoxosternite (Fig. 10B).
prfs	Prefemur-syncoxosternite m.	Arises on posteroproximal margin of prefemur of leg 1 lateral to *prfr;* passes proximally; inserts on syncoxosternite just in from proximal margin (Fig. 10B).
fel	Femur levator m. = levator femoris (M)	Arises on dorsoproximal corner of femur; passes proximally deep to *fed;* inserts proximally on prefemur (Figs. 9, 10A, C, E).
fed	Femur depressor m. = depressor femoris (M)	Arises on ventroproximal corner of femur; passes proximally superficial to *fel;* inserts proximally on anterior and posterior faces of prefemur (Figs. 9, 10A, C, E).
fer	Femur retractor m. = retractor femoris (M)	Arises on posteroproximal margin of femur; passes proximally superficial to *fed;* inserts on posterodistal surface of prefemur (Figs. 9, 10B, C, E–F).
pff	Postfemur flexor m. = flexor postfemoris (M)	Arises on ventroproximal corner of postfemur; passes proximally; inserts on femur proximally (Fig. 9).
tif.fe	Femural head of tibial flexor m. = posterior part of flexor tibiae (M)	Arises on ventroproximal corner of tibia; passes proximally; inserts on dorsal surface of femur (Fig. 9).
tif	Tibial flexor m. = flexor tibiae (M)	Arises on ventroproximal corner of tibia; passes proximally; inserts on posterior and dorsal surfaces of postfemur (Fig. 9).
ptf.pf	Postfemural head of posttarsal flexor m.	Arises on long tendon from ventroproximal corner of posttarsus; passes dorsoproximally; inserts on dorsodistal surface of postfemur (Fig. 9).
ptf.ti	Tibial head of posttarsal flexor m. = flexor unguiculi (M)	Arises on long tendon from ventroproximal corner of posttarsus; passes dorsoproximally; inserts on dorsal surface of tibia (Fig. 9).
Gonopod muscles		
gp1	Medial apodeme-coxa m. = m. 1 trachéo-coxal des gonopodes (D)	Arises on the distal-medial face of the apodeme; passes ventrally; inserts on the medial margin of the gonopod coxa (Figs. 5A, 6A, 7A–C).
gp2	Apodeme-tergal m.	Arises on the anterior face of the gonopod apodeme arm; passes dorsally shallow to *pt2;* inserts on T7 dorsolaterally posterior to phragma (Figs. 5A–B, 6A–B, 7A, C–D).
gp3	Posterior apodeme-coxa m. = m. trachéo-télopodial m. (D)	Arises on gonopod apodeme base posteriorly; passes distally; inserts on posterior face of gonopod apodeme arm proximal to *gp4* (Figs. 5B–C, 6B, 7A–C).

TABLE 1. (Continued)

No.	Name	Direction
Gonopod muscles (continued)		
gp4	Lateral apodeme-coxa m. = m. 2 trachéo-coxal des gonopodes (D)	Arises on the distal-lateral face of the apodeme; passes ventrally; inserts on the anterolateral corner of the gonopod coxa (Figs. 5B–C, 6B, 7A–C).
gp5	Intrinsic coxal m. = m. paracoxite-base coxale du télopodite (D)	Arises at base of gonopod coxal flange; passes proximally; inserts on lateral bar of gonopod apodeme base (Figs. 6B, 7A–D).
gp6	Ventral coxa-t6 m.	Arises on the anterior of the gonopod coxa proximally; passes anteriorly shallow to *va2* and *pt4;* inserts on the phragma of t6 ventrolaterally (Fig. 6B).
gp7	Dorsal coxa-t6 m.	Arises on the anterior of the gonopod coxa proximally; passes anterodorsally shallow to *va2* and deep to *pt4;* inserts on the phragma of t6 laterally (Figs. 6A–B).
gp8	Leg 9-gonopod apodeme m.	Arises on the vestige of leg 9; passes dorsally; inserts on gonopod apodeme arm distally (Figs. 5A–B).
gp9	Apodeme-posterior gonopod m.	Arises on the vestige of leg 9; passes posterodorsally deep to *pt4* and shallow to *va1;* inserts on the phragma of t8 anteriorly (Figs. 5A–C).
gp10	Posterior gonopod-t8 m.	Arises on the vestige of leg 9; passes posteriorly deep to *pt4;* inserts on the anterior ventral apodeme of t8 (Fig. 5A–D).
gp11	Leg 9-pleurotergite m.	Arises on the vestige of leg 9; passes dorsolaterally deep to *pt4* and shallow to gonopod apodeme arm; inserts on t7 laterally (Fig. 5C–D).

*The name proposed for each muscle is derived from anatomical characteristics such as the origin, insertion, and fiber direction. To facilitate cross-referencing, the names given to muscles in *Plusioporus salvadorii* by Silvestri (1903) and in *Poratophilus punctatus* by Manton (1954, 1958, 1961, 1964) are denoted by (S) and (M), respectively. Names given to gonopod muscles by Demange (1967) are denoted by (D).

Phyllogonostreptus nigrolabiatus, a spirostreptidan millipede, belongs to the Juliformia, a group characterized by the possession of ring-shaped trunk segments, together with the spirobolidans and julidans. The Juliformia is one of the most intensively studied millipede groups due to the relatively large size and abundance of its members. However, taxonomic studies far outnumber those from an anatomical perspective and many aspects of juliform skeletomuscular anatomy, and that of millipedes in general, remain poorly known. Most previous studies of millipede skeletomuscular anatomy, particularly that of juliforms, have focused on limited areas of the body. Fechter (1961) described the cephalic skeletomuscular anatomy of *Cylindroiulus teutonicus* (= *C. caeruleocinctus*) (Julida) and Manton (1964) described those elements of the cephalic musculature of *Poratophilus punctatus* (Spirostreptida) associated with the mandibles and tentorium. Manton (1961) surveyed the midbody trunk musculature across a range of millipede orders, including those belonging to the Juliformia. The only work that has more comprehensively surveyed juliform musculature is that of Silvestri (1903), in which he described the cephalic, collum, midbody trunk, and appendicular musculature of the spirostreptid *Plusioporus salvadorii*. However, Silvestri did not include skeletomuscular descriptions of the gonopods or anteriormost or posteriormost trunk rings. The musculature of spirostreptid gonopods has only previously been published by Demange (1964, 1967); however, the illustrations are so overly schematic as to be nearly impossible to interpret.

It has long been appreciated that the first three leg-bearing segments in millipedes differ from the following rings, the obvious distinction being that they bear only a single pair of legs as opposed to the double pair diagnostic of millipedes. These anteriormost rings are sometimes collectively referred to as the "thorax." An obvious exception to the pattern described above is found in the Spirobolida, where the first five trunk segments, including the collum, appear to bear a single pair of legs each. However, it has been shown that this distribution is due to the anterior shift of appendages 1–4 from the typical millipede position during development (Bodine, 1970). In spite of the fact that the thoracic rings of millipedes bear only a single pair of appendages, they have been suggested to be diplosegments, as in the remainder of the trunk. Various hypotheses addressing this claim have been based on additional skeletomuscular characters that distinguish the thoracic from the postthoracic rings. However, previous interpretations of these characters with regard to the segmental composition of the millipede thorax were made before the advent of parsimony-based phylogeny. Thus, a reevaluation of these characters within the current parsimony-based millipede phylogenetic framework is conducted here in order to evaluate the support for earlier hypotheses. This evaluation, in combination with the evidence gained from an exhaustive survey of the skeletomuscular anatomy of the spirostreptid *Phyllogonostreptus nigrolabiatus*, has lead to the formulation of a new hypothesis: the musculature of the postthoracic diplosegments is derived relative to that of the thoracic segments which are haplosegments.

MATERIALS AND METHODS

Twenty specimens of adult male and female *Phyllogonostreptus nigrolabiatus* (Newport, 1844)

(Spirostreptida: Harpagophoridae) were obtained preserved in Wardsafe® from Ward's Natural Science Establishment. The millipedes are sold by Ward's as "*Spirobolus*" and were identified as *P. nigrolabiatus* by Richard Hoffman, Virginia Museum of Natural History. Specimens averaged 130 mm in length and 4 mm in diameter. Specimens were dissected under 95% ethanol using both transmitted and reflected light. Drawings were made with the aid of a camera lucida attachment, digitized using a scanner, and finally traced and labeled using Adobe Illustrator®. The origin, insertion, and relative position was documented for each muscle. Using this information the cephalic muscles were compared with those described in the millipede *Cylindroiulus teutonicus* (Pocock, 1900) (= *C. caeruleocinctus* (Wood, 1864)) (Julida: Julidae) by Fechter (1961) and homologies were proposed.

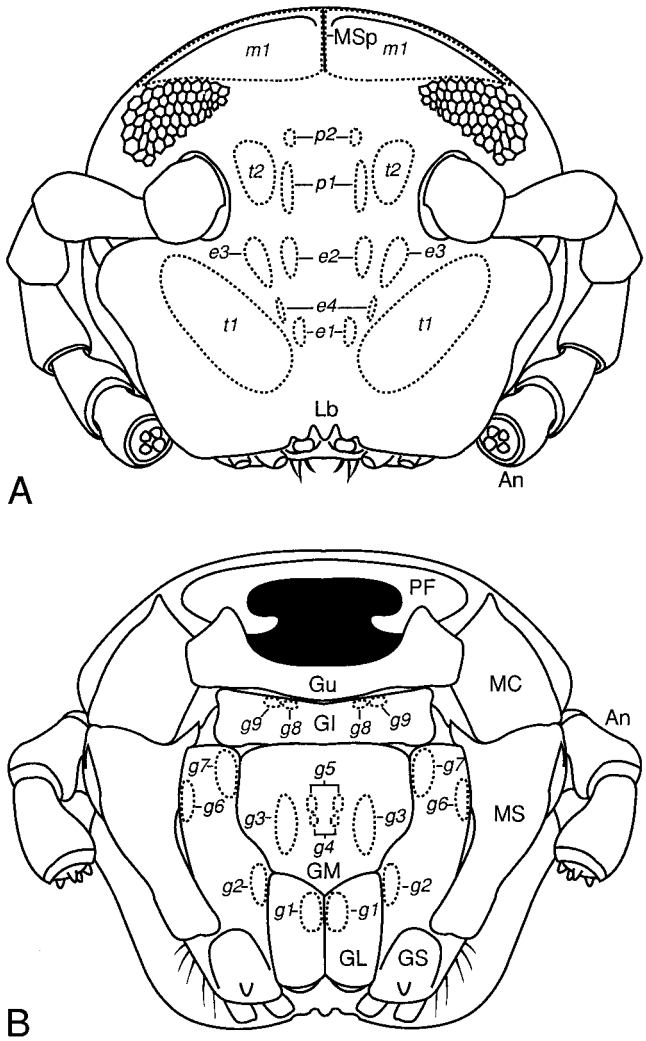

Fig. 1. *Phyllogonostreptus nigrolabiatus*. Dorsal (**A**) and ventral (**B**) views of the external cephalic skeleton with the areas of muscle attachment indicated by dashed lines. Muscle abbreviations are defined in Table 1. An, antenna; GI, gnathochilarial intermentum; GL, gnathochilarial lingual lobe; GM, gnathochilarial mentum; GS, gnathochilarial stipes; Gu, gula; Lb, labrum; MC, mandibular cardo; MS, mandibular stipes; Msp, median septum; PF, postoccipital flange.

RESULTS

A comprehensive list of the muscles occurring in *Phyllogonostreptus nigrolabiatus* is presented in Table 1. The muscles are named based on their position in the body, rather than on their function, so as not to hypothesize functional qualities that have not been tested in this study. To facilitate cross-referencing, the names given to spirostreptid muscles previously described in the literature are also given.

Cephalic Musculature

In all but one detail the cephalic musculature determined for *Phyllogonostreptus nigrolabiatus* (Figs. 1–3) agrees with that described by Silvestri (1903) for the spirostreptid *Plusioporus salvadorii* (Table 1). *Plusioporus salvadorii* belongs to the Spirostreptidae (which together with the Harpagophoridae form the superfamily Spirostreptoidea), indicating interfamilial conservation of cephalic musculature. Silvestri (1903) described a small muscle, depressor tendinous subpharingei, running from the mentum to the transverse tendon and which has its origin in the same position as *g5* in *P. nigrolabiatus*, which runs from the mentum to the top of the hypopharyngeal furrow (Figs. 1B, 2D, 3A). It seems possible that Silvestri misidentified the insertion point of this muscle as the transverse tendon instead of the hypopharynx.

Thorax and Midbody Trunk Musculature

The midbody trunk musculature (Fig. 4) and that of the associated appendages (Fig. 9) determined for *Phyllogonostreptus nigrolabiatus* is in general agreement with that previously described in *Plusioporus salvadorii* (Silvestri, 1903; Manton, 1958) and *Poratophilus punctatus* (Harpagophoridae) (Manton, 1954, 1961). However, the musculature of the first three postcollum rings (t2–t4) has not previously been described. Portions of this musculature were figured by Demange (1967) for an unidentified spirostreptidan; however, the illustrations were so diagrammatic as to make determination of exact origin and insertion points of the muscles impossible. Trunk rings 2–4 each bear only a single pair of appendages, in comparison to the rest of the podous trunk rings that bear two pairs each (Fig. 5). The first three pairs of legs in *P. nigrolabiatus* show little variation between males and females and are modified relative to the following legs in several ways. In leg pairs one and two the coxa (and presumably the trochanter) are fused with the sternite to form a syncoxosternite (Fig. 10A–D). The ventral apodemes are elongate, upright (Fig. 9), and do not meet on the

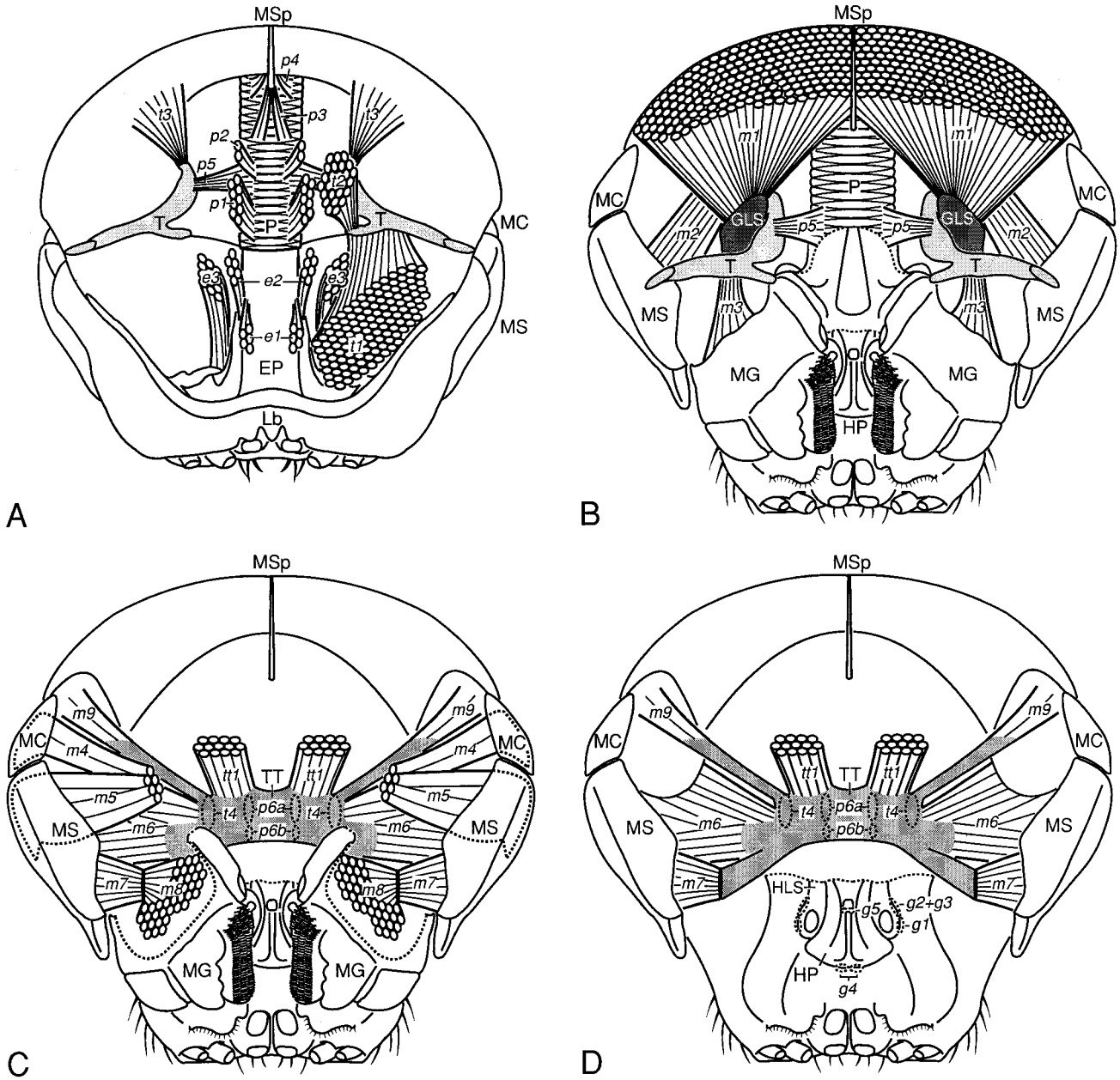

Fig. 2. *Phyllogonostreptus nigrolabiatus*. Serial dissection of cephalic skeletomuscular anatomy in dorsal view. **A**: Antennae, frons, and clypeolabrum removed and showing pharyngeal, tentorial, and epipharyngeal musculature. Mandibular muscle *m1* has been removed so as not to obscure tentorial muscle *t3*. **B**: Epipharynx removed to reveal mandibles and portions of hypopharynx. **C**: Pharynx, tentorium, and proximal portion of mandibular gnathal lobe removed to reveal transverse tendon. **D**: Mandibular gnathal lobes removed to show hypopharynx. Muscle abbreviations are defined in Table 1. EP, epipharynx; GLS, gnathal lobe sclerite; HP, hypopharynx; LB, labrum; MC, mandibular cardo; MG, mandibular gnathal lobe, MS, mandibular stipes; MSp, median septum; P, pharynx; T, tentorium; TT, transverse tendon.

midline as in all the following rings. Rings 2–4 have all of the muscles present in the midbody rings (Fig. 4) in addition to muscles that are unique to these anteriormost rings. The unique muscles are found among the ventral apodeme muscles and the extrinsic and intrinsic leg muscles.

Ventral apodeme muscles *va3, va4, vg, vh,* and *vc* (Figs. 5, 10) occur uniquely in the thorax. Muscle *va3* runs from the distal end of the ventral apodeme to the dorsolateral wall of the pleurotergite of the same ring and *va4* runs from the ventral apodeme to the anteromedial corner of the pleurotergite of the same ring. Muscles *vg, vh*, and *vc* are unique to the ventral apodeme of ring 2 (leg 1) and run to the gula, head, and collum, respectively. In addition, *va1* is split into dorsal and ventral components (Fig. 5A–C).

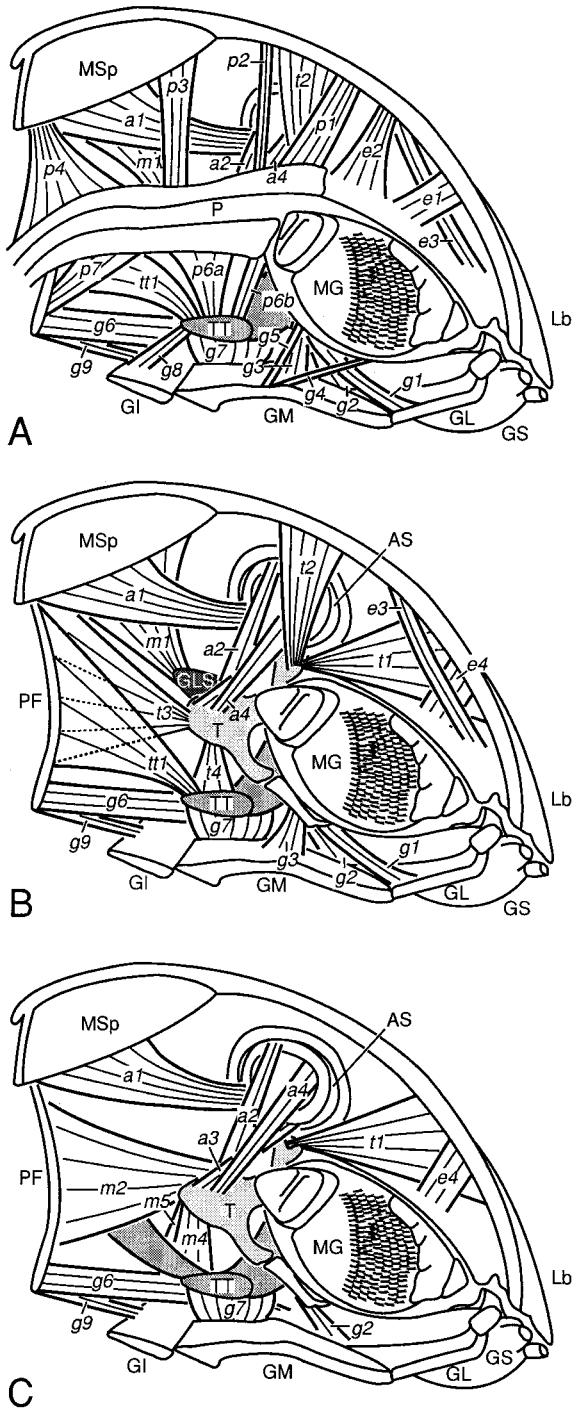

Fig. 3. *Phyllogonostreptus nigrolabiatus*. Serial dissection of cephalic skeletomuscular anatomy in sagittal view with the deepest muscles shown in **A**, the pharynx removed in **B**, and the shallowest muscles shown in **C**. Muscle abbreviations are defined in Table 1. AS, antennal socket; GI, gnathochilarial intermentum; GL, gnathochilarial lingual lobe; GLS, gnathal lobe sclerite; GM, gnathochilarial mentum; GS, gnathochilarial stipes; Lb, labrum; MG, mandibular gnathal lobe; MSp, median septum; P, pharynx; PF, postoccipital flange; T, tentorium; TT, transverse tendon.

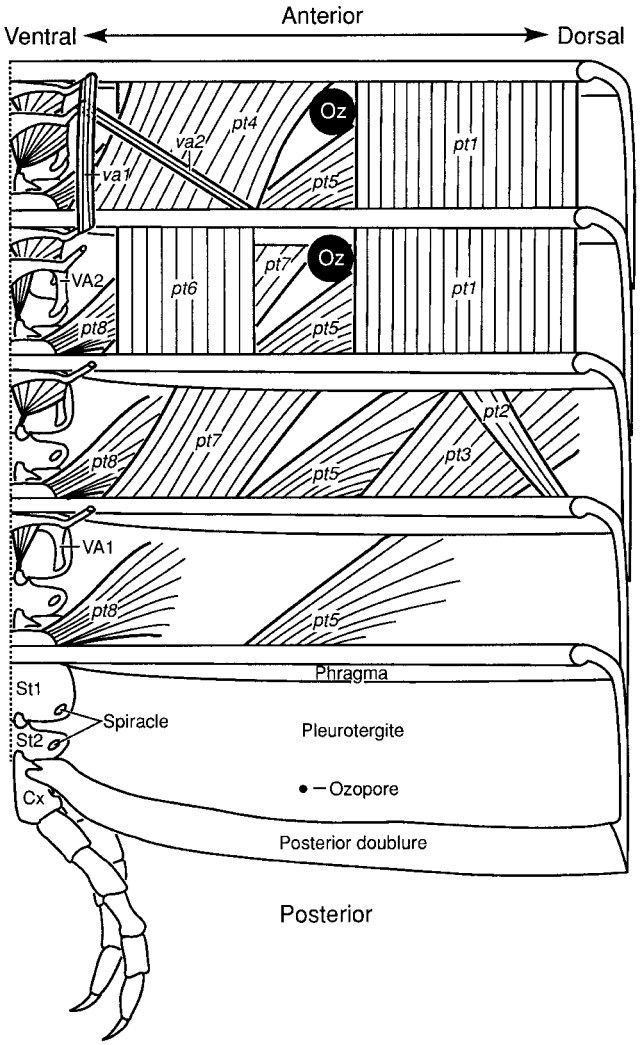

Fig. 4. *Phyllogonostreptus nigrolabiatus*. Skeletomuscular anatomy of midbody trunk rings spread open from ventral to dorsal midlines. Deep musculature is shown in the anteriormost ring illustrated and layers of muscles are removed in each of the successive rings to reveal the more superficial musculature. Ozadenes removed on all but the two anteriormost rings. Muscle abbreviations are defined in Table 1. Cx, coxa; Oz, ozadene; Sp, spiracle; St1, anterior sternite; St2, posterior sternite; VA1, anterior ventral apodeme; VA2, posterior ventral apodeme.

Unique to appendages 1 and 2 is a muscle, *spt*, which runs from the lateral corner of the sternite to the pleurotergite of the same ring (Figs. 5C–D, 10A,C). A pair of small sclerites, generally referred to as intercalary sclerites (is), occurs posterior to leg pairs 1–3 in the intersegmental membrane (Fig. 10B,D,F). The only muscle serving this sclerite, *isp*, runs from the posterolateral corner of the intercalary sclerite to the pleurotergite of the same ring (Figs. 5B,D, 10B,D,F).

The intrinsic leg musculature of legs 1–3 is generally the same as that of unmodified appendages, but with no musculature representative of the coxa (which has been fused with the sternite) and

with the presence of prefemur flexor, *prfr*, and prefemur–syncoxosternite, *prfs*, muscles in leg 1 (Fig. 10).

The extrinsic musculature of legs 1–3 deviates from the pattern present in unmodified legs (Fig. 4). Leg 3 has both a retractor muscle, *ar*, and a protractor muscle, *ap*, running from the proximal margin of the coxa to the ventral apodeme (Fig. 10E,F). Leg 2 has only the protractor muscle, *ap* (Fig. 10C), and leg 1 lacks both *ar* and *ap* (Fig. 10A,B). However, there is a pair of extrinsic leg muscles that is unique to legs 1–3: *ova* and *ova*^{c}. Both *ova* and *ova*^{c} attach to the distal end of the leg 1 ventral apodeme posteriorly and pass posteroventrally to attach to the anterior margin of the leg 2 syncoxosternite, with *ova*^{c} crossing (Figs. 5A,B, 10A–C). Muscles *ova* and *ova*^{c} also run from the distal end of the leg 2 ventral apodeme posteriorly to the anteroproximal margin of the coxa of leg 3 (Figs. 5A,B, 10E). A chiasmatic muscle pair, *og*, runs from the anterior margin of the leg 1 syncoxosternite to the gula (Figs. 5A, 10A,B).

Posterior Musculature

The musculature associated with the posterior trunk rings, telson, and the anal valves in millipedes has not previously been documented. In *Phyllogonostreptus nigrolabiatus* the final trunk ring, the preanal ring (PR), is apodous (Fig. 8A,B). This ring is part of the telson and is apodous in all millipedes, as it is posterior to the proliferation zone for addition of new segments during ontogeny. While the adults of *P. nigrolabiatus* have two pairs of appendages on the penultimate trunk ring (t^0), in early juvenile stadia of spirostrepitdans (and in adults of some taxa) there are a number of legless diplosegments between the last leg-bearing segment and the telson (Enghoff et al., 1993). Dorsally, the preanal ring is extended posteriorly into an upturned point, the epiproct (epi), and ventrally the preanal ring articulates with a small triangular sclerite, the anal plate (AP). Laterally, the preanal ring articulates with the paired anal valves (AV). An eversible anal sac (EAS), which attaches to the posterior margin of the anal valves, is continuous with the anus (As) (Fig. 8A). The musculature of ring t^{-1} (Fig. 8A,B) is identical to that of a typical midbody trunk segment (Fig. 4). The musculature of the penultimate ring, t^0, is nearly identical, lacking only muscle *va1* (Fig. 8A,B). A set of muscles, *av1* and *av2*, runs from the posterolateral and ventrolateral portion of the preanal ring phragma to the dorsomedial and ventromedial corners of the anal valve, respectively. Also originating on the preanal ring phragma are two anal dilators, *ad2* and *ad1* (Fig. 8B). Numerous thin muscles run from the phragma of the preanal ring to the eversible anal sac (*esm*) or the junction between the sac and the anal valves (*esl*).

Gonopod Musculature

As first noted by Brölemann (1916), in the suborder Spirostreptidea the gonopods are formed only by leg pair eight, the ninth pair being almost completely reduced (Brölemann, 1935; Demange, 1964, 1967). The gonopods (Fig. 7) are traditionally described as consisting of the following elements: sternite (St), coxa (Cx), flagelliform telopodite (Te), and apodeme (Ap). In the Harpagophoridae the proximal portion of the telopodite is completely enclosed by the coxa, with the telopodite exiting the coxa posteriorly (Fig. 7C,D). The coxae are in contact medially and are joined to a small anterior sternite (St). A dorsolateral extension of the coxa is fused with the proximal end of the telopodite, forming an arch, the apodeme base (Ab), upon which the gonopod apodeme arm (Aa) articulates in a small socket. There is only one intrinsic gonopodal muscle, *gp5*, which runs from the posterior flange of the coxa (Cxf) to the apodeme base (Figs. 6B, 7). No muscles insert on the telopodite. When the gonopod is retracted, the apodeme base points anterodorsally, the apodeme arm is folded towards the coxa, and muscle *gp2* is loose (Fig. 5A,B). When the gonopod is extended, the apodeme base and arm are aligned and muscle *gp2* is taut (Fig. 6). At present, it is not possible to homologize the gonopod muscles with the intrinsic muscles of unmodified appendages with any certainty.

A hinged gonopodal apodeme is not unique to the Spirostreptida, occurring also in some Spirobolida, although on the posterior gonopod (Hoffman, 1982), and as such the two apodemes are not homologous. The musculature associated with this hinge mechanism is described for the atopetholid spirobolidan *Atopetholus angelus* by Hoffman and Orcutt (1960). A third type of hinged gonopodal apodeme is found in the Paectophyllini, a tribe of Julidae, where the apodeme of the posterior gonopod is connected to the mesomerite along a broad articulation (Enghoff, 1985).

The gonopods of *Phyllogonostreptus nigrolabiatus* are connected to leg pair nine and to rings seven and eight by a large membranous sac, most of which is not shown in Figs. 5 and 6 so as not to obscure other structures. Leg pair nine is represented only by a pair of small, triangular sclerotizations in the gonopodal sac, although these sclerotizations retain some musculature (Fig. 5A–D). Some possible homologies can be suggested for this associated musculature, assuming that the ventral apodeme associated with leg 9 before modification has been incorporated into the remnant sclerite. Under this assumption, muscles *gp8* and *gp10* may be homologous to *va1*. In midbody trunk rings the majority of the fibers in *va1* run from the anterior ventral apodeme of one diplosegment to the anterior ventral apodeme of the following diplosegment. However, there are a few fibers that run from the posterior

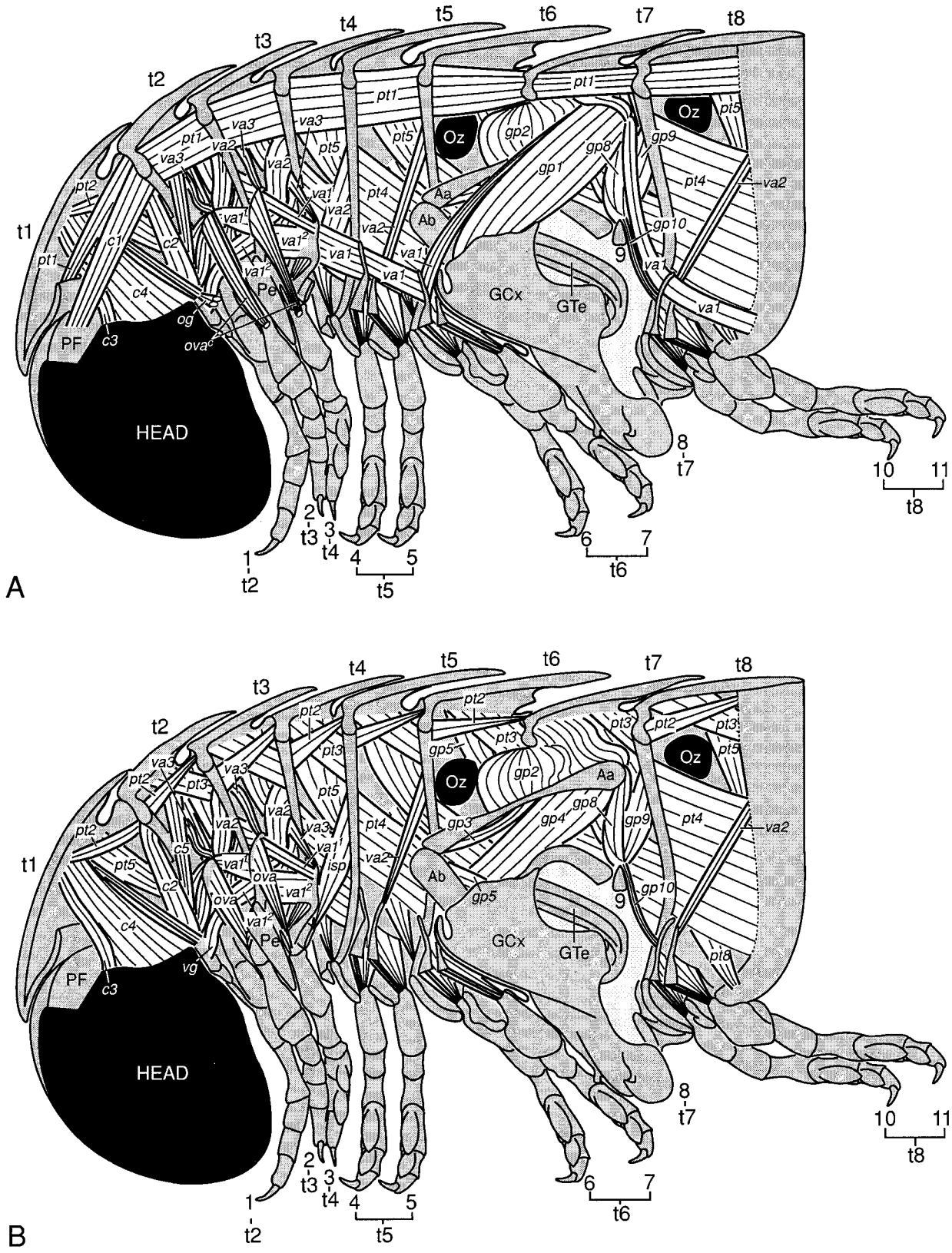

Figure 5

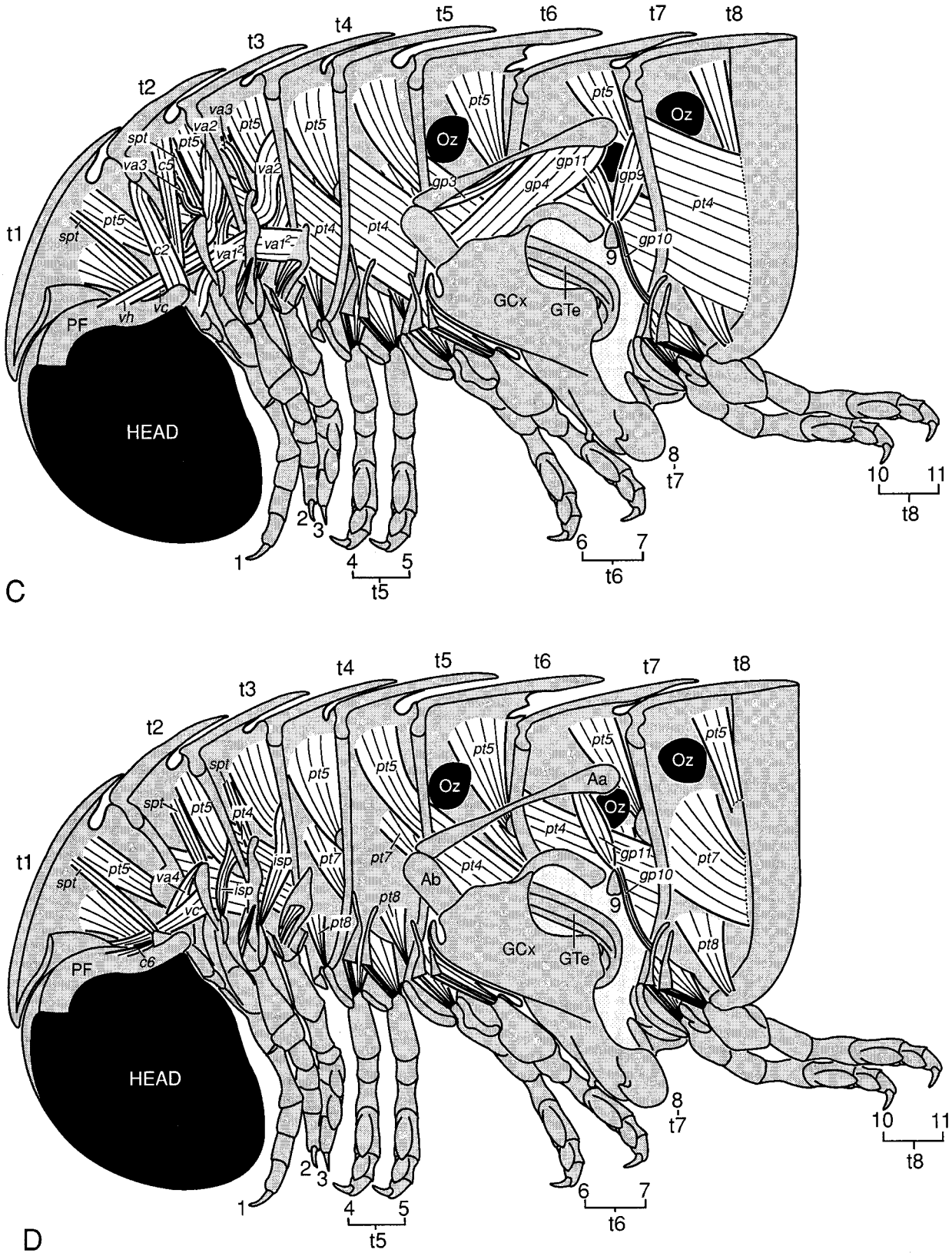

Fig. 5. *Phyllogonostreptus nigrolabiatus*. Serial dissection of anterior trunk rings 1–8 of a male in sagittal section with gonopod retracted. Most of the membrane connecting the gonopod to the trunk pleurotergites is not shown for clarity. **A**: Deepest musculature. **B**: *c1* and *pt1* removed dorsally, *va1* removed ventrally except on t2–t4, *gp1* removed to reveal more superficial gonopod musculature. **C**: *c3* and *c4* removed from collum; *pt2* and *pt3* removed dorsally, *va2* removed except in t2–t3, $va1^1$ *removed, gp8* removed to reveal *gp11*. **D**: *c2*, *c5*, and *vh* removed from collum, $va1^2$ *and va2* removed from anterior rings to reveal *isp*, *pt4* removed except in t2–t3 and t6–t7 to reveal *pt6* and *pt7*, *gp4* and *gp9*, removed. Muscle abbreviations are defined in Table 1. Aa; gonopod apodeme arm; Ab, gonopod apodeme base; GCx, gonopod coxa; GTe, gonopod telopodite; Oz, ozadene; Pe, penis; PF, postoccipital flange; t, tergite.

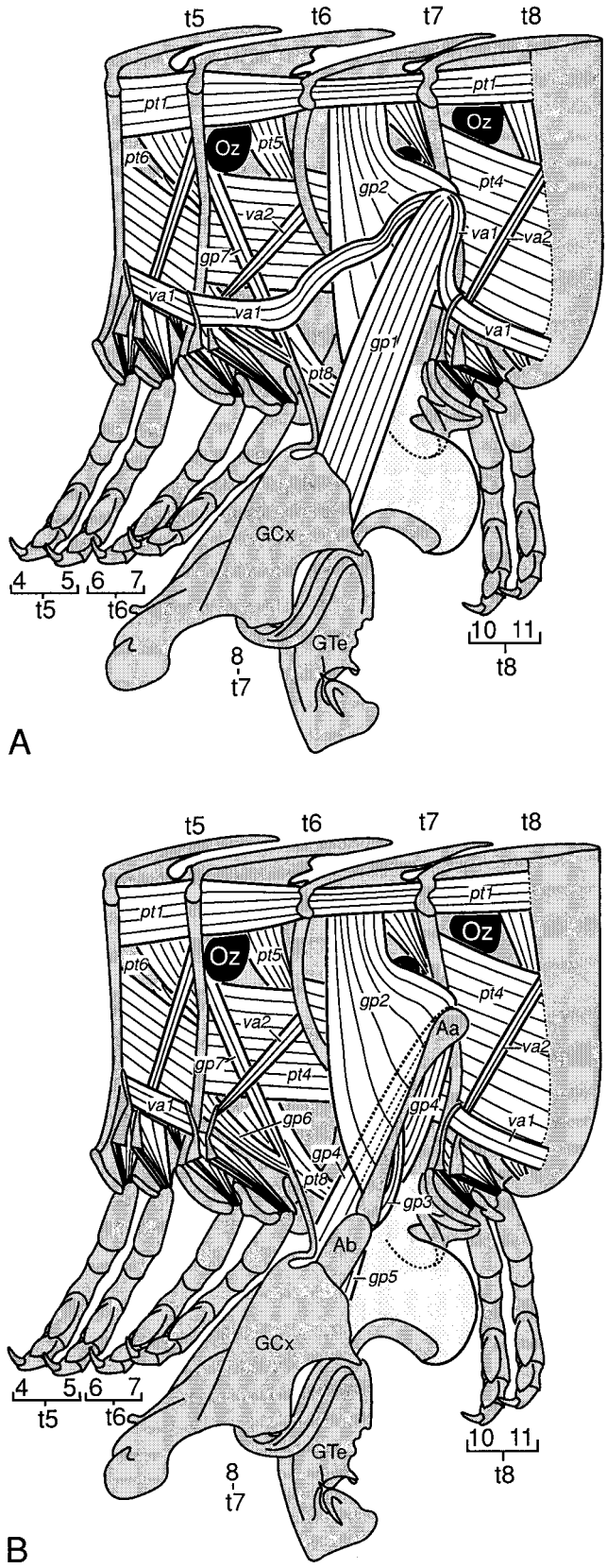

Figure 6

ventral apodeme of one diplosegment to the anterior ventral apodeme of the following diplosegment, and a few fibers that run from the anterior to the posterior ventral apodeme within a diplosegment. Based on its origin from a modified posterior appendage and its insertion on the lateral portion of the phragma, *gp9* may be homologous to *va2*.

Demange (1967) stated that all harpagophorids have *gp1* and *gp4* (muscle trachéo-coxal des gonopodes 1 and 2) combined to form a continuous sheet that encircles the base of the coxa. However, this is not the case in *Phyllogonostreptus nigrolabiatus*, where the two muscles are separate (Fig. 7A–C), as described by Demange (1967) for the Spirostreptidae. Demange (1967) also claimed that a transverse muscle connecting the apodemes of a pair of gonopods is universally present. However, no evidence for such a muscle is found in *P. nigrolabiatus* and, additionally, no such muscle was described in the spirobolidan *Atopetholus angelus* by Hoffman and Orcutt (1960).

Comparison of Spirostreptidan and Julidan Cephalic Muscular Anatomy

Fechter (1961) exhaustively detailed the cephalic musculature of the julidan millipede *Cylindroiulus teutonicus* (= *C. caeruleocinctus*), the only non-spirostreptidan millipede for which the cephalic musculature has been documented in such detail. A comparison of the musculature between the two taxa (Table 2) reveals that, while there are many conserved muscles as identified by similar points of origin and insertion, there are some interordinal differences. There are no homologs for muscles *e4, g3, g5, g8, g9, m3,* and *m7* of *Phyllogonostreptus nigrolabiatus* in *C. teutonicus*. There are no muscles described in *C. teutonicus* for which there lack homologs in *P. nigrolabiatus*. Muscle *e4*, the anterolateral epipharyngeal muscle, is very thin and, as

Fig. 6. *Phyllogonostreptus nigrolabiatus*. Skeletomuscular anatomy of trunk rings 5–8 of a male with gonopod extended. Vestigial appendage 9 and its associated musculature are not shown for clarity. **A**: Sagittal section showing deepest musculature. **B**: Same as above with *va1* removed from rings 6–7 and *gp1* removed from the gonopod to reveal *gp3* and *gp4*. Muscle abbreviations are defined in Table 1. Aa, gonopod apodeme arm; Ab, gonopod apodeme base; GCx, gonopod coxa; GTe, gonopod telopodite; Oz, ozadene; t, tergite.

Fig. 7. *Phyllogonostreptus nigrolabiatus*. Gonopod skeletomuscular anatomy. **A**: Anterior view. **B**: Same as above with *gp2* removed to reveal insertion points of *gp1* and *gp4*. **C**: Posterior view. **D**: Same as above with *gp1* removed to reveal insertion point of *gp3*, *gp4* removed to reveal base of *gp2* and the coxal flange removed to show *gp5*. Muscle abbreviations are defined in Table 1. Aa, gonopod apodeme arm; Ab, gonopod apodeme base; Cx, gonopod coxa; Cxf, gonopod coxal flange; Tl, gonopod telopodite.

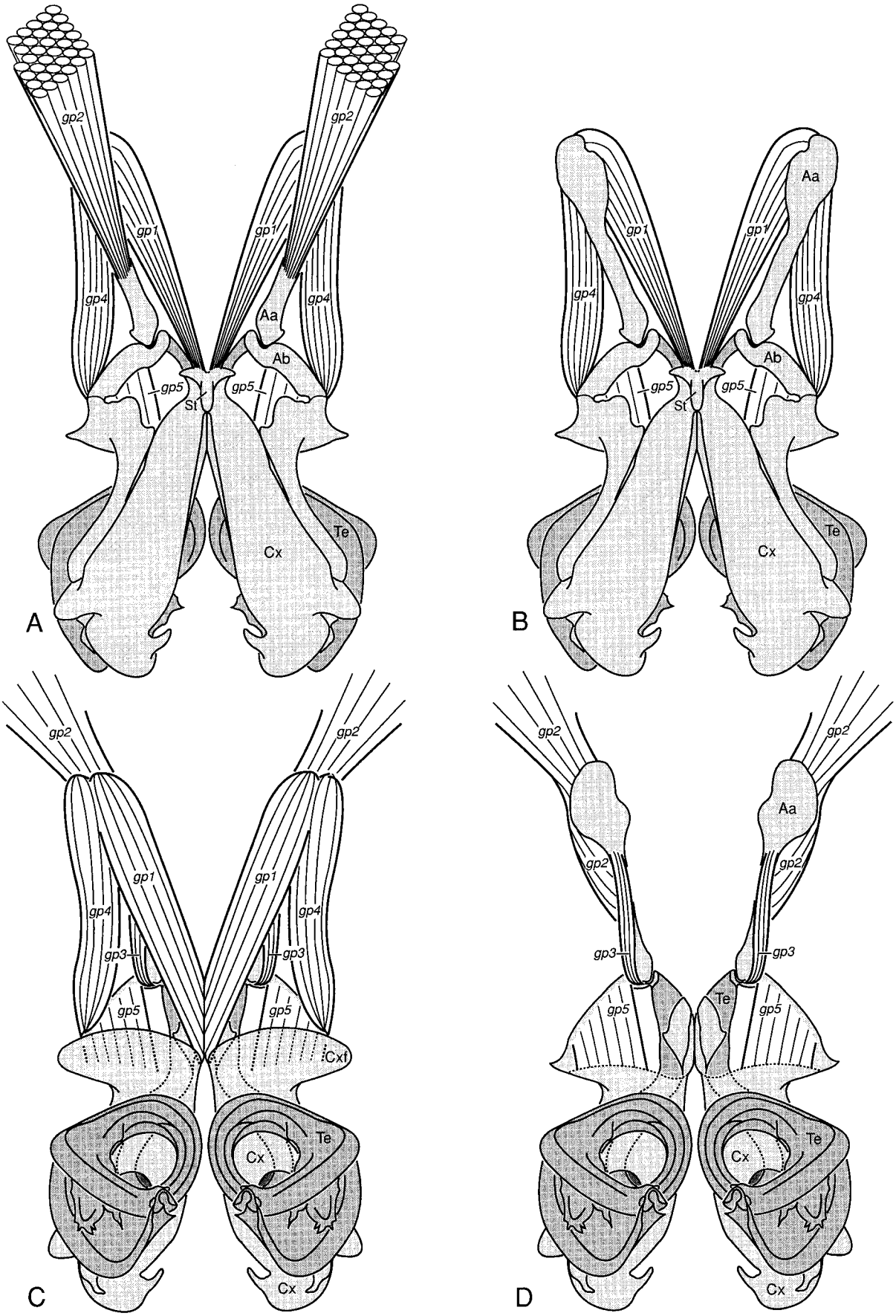

Figure 7

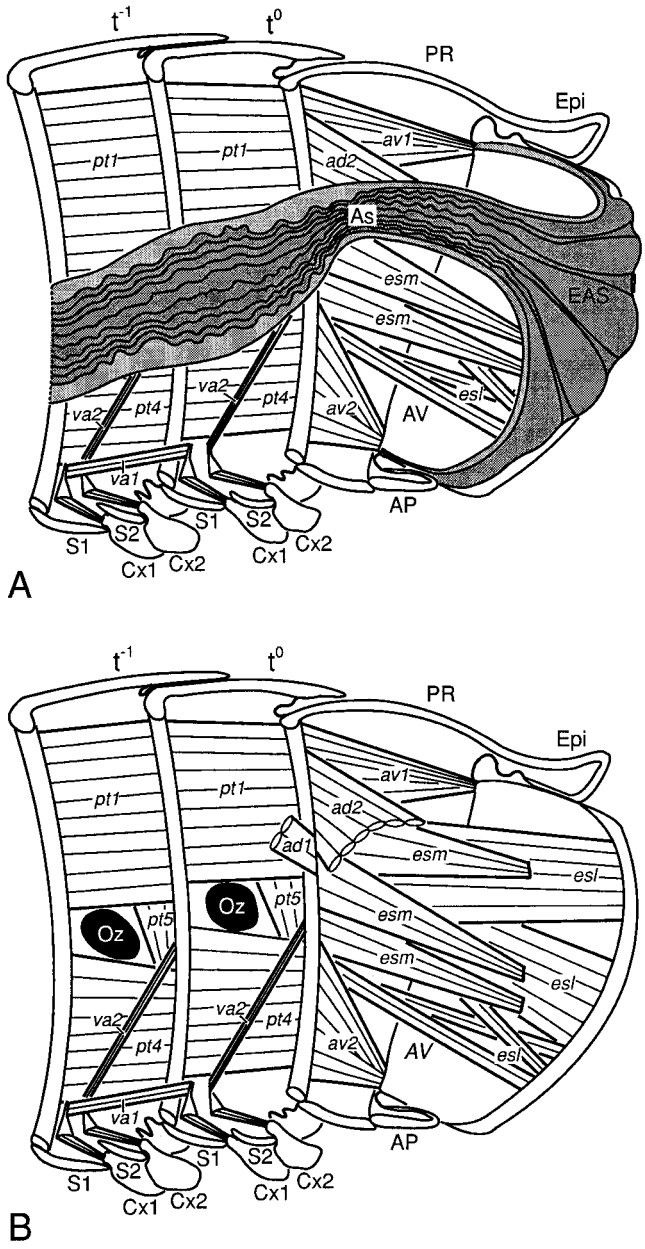

Fig. 8. *Phyllogonostreptus nigrolabiatus*. Posterior trunk skeletomuscular anatomy. **A**: Sagittal section through the posteriormost two trunk rings and the telson including the gut; distal portions of the appendages are not shown. **B**: Same view as above but with the gut removed. Muscle abbreviations are defined in Table 1. As, anus; AP, anal plate; AV, anal valve; Cx, coxa; EAS, eversible anal sac; Epi, epiproct; Oz, ozadene; PR, preanal ring; S, sternite; t, tergite.

Fechter (1961) may have overlooked it, its absence in julidans will need to be confirmed through further study. The majority of the remaining muscles with no homolog in *C. teutonicus* are gnathochilarial. The form of the gnathochilarium differs distinctly between spirostreptidans and julidans and is one of the more obvious characters which is used to diagnose the two orders. In julidans, the gnathochilarial stipes are in contact along most of their posterior half, as opposed to being separated by the mentum, as in spirostreptidans (e.g., Fechter, 1961, fig. 2; Jeekel, 1985, fig. 2) and most other Chilognatha except some of the specialized Colobognatha (Silvestri, 1903; Hoffman, 1982). This symphyognathous condition is generally accepted to be derived (Verhoeff, 1911; Enghoff, 1981, 1991; Jeekel, 1985), and Jeekel (1985) postulated that the ancestral juliform condition consisted of three pairs of medial sclerites (lingual lobes, promental, and mental sclerites) and a pair of large lateral sclerites, the gnathochilarial stipes. These muscular differences highlighted in a limited comparison of taxa from two closely related millipede orders suggest the potential utility of comparative anatomical studies for resolving millipede phylogeny.

DISCUSSION

The first three postcollum rings, forming what is sometimes referred to as the diplopod "thorax," have only a single pair of legs each, while the following rings each have two pairs of legs. This gives the immediate impression that the first three postcollum rings are each derived from a single somite. However, the segmental nature of the thorax has been subject to debate, with one camp (e.g., Latzel, 1884; Silvestri, 1903; Brölemann, 1935; Dohle, 1964, 1974; Bodine, 1970; Enghoff et al., 1993) supporting the hypothesis that these rings are haplosegments, and the other supporting the hypothesis that these rings actually represent diplosegments, even though they each bear only one pair of appendages (e.g., Verhoeff, 1926–1932; Pflugfelder, 1932; Demange, 1967; Kraus, 1990). The evidence used to support both arguments has come from skeletal, muscular, and other soft-tissue anatomy and is critically reviewed below. In addition, prompted by the anatomy of *Phyllogonostreptus nigrolabiatus* and other millipede taxa, a novel hypothesis concerning the phylogenetic evolution of juliform musculature is posited.

The musculature of the first three postcollum trunk rings in many millipedes, as illustrated by *Phyllogonostreptus* (Figs. 4, 5), is considerably more complex than those which make up the rest of the trunk. Manton (1961) used the greater muscular complexity of juliform thoracic rings in comparison to postthoracic rings to argue for thoracic diplosegments. She reasoned that this complexity resulted from the retention of muscles that would have served two appendages in a diplosegment with one pair of the appendages suppressed. For example, in the thorax of the chordeumatidan *Polymicrodon* both the levator apophyses anticae (*va3*) and the levator apophyses posticae (*va1*) attach to a single ventral apodeme, whereas in the postthoracic diplosegments these muscles are distributed between two ventral apodemes (Manton, 1961, text, figs. 26–27). In Manton's scenario, this doubling-up of mus-

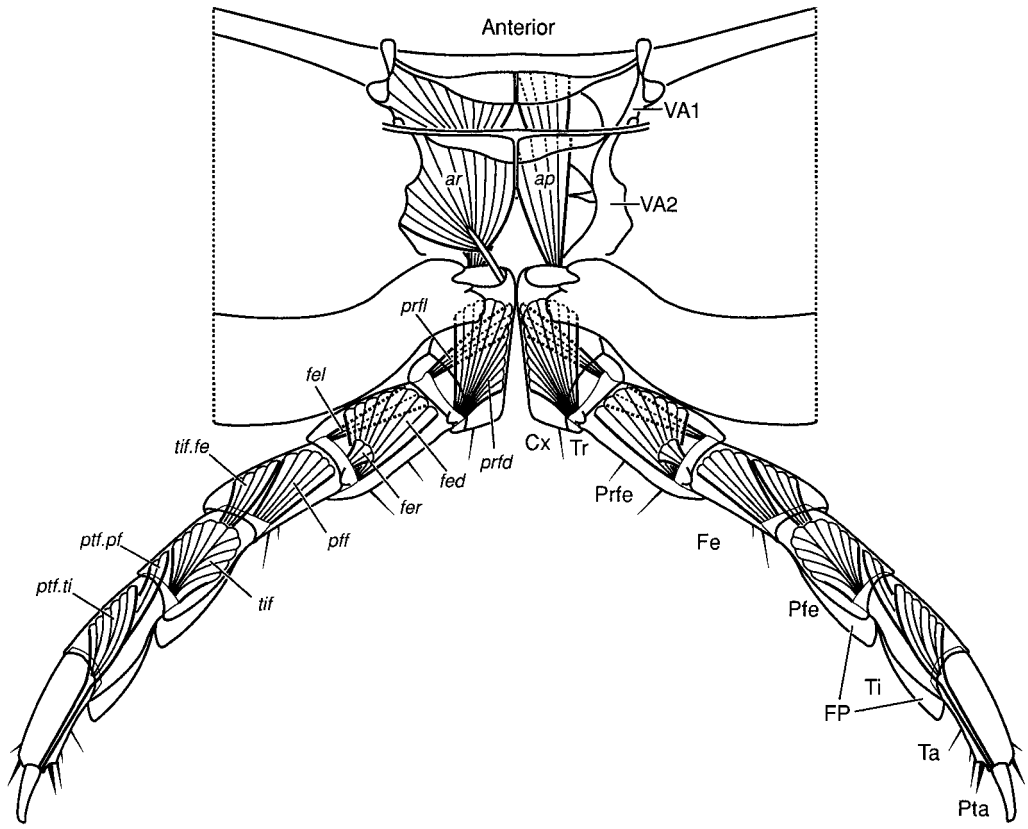

Fig. 9. *Phyllogonostreptus nigrolabiatus*. Skeletomuscular anatomy of the posterior pair of appendages on a midtrunk segment, with most of the pleurotergal ring removed, in posterior view. The musculature of the anterior pair of appendages is identical. Muscle *ar* is removed on the right side of the figure to reveal *ap*. Muscle abbreviations are defined in Table 1. Cx, coxa; Fe, femur; FP, fleshy pad (found on males only); Pfe, postfemur; Prfe, prefemur; Pta, posttarsus; Ta, tarsus; Ti, tibia; Tr, trochanter; VA1, anterior ventral apodeme; VA2, posterior ventral apodeme.

cles was the result of the loss of a sternite and a leg pair in each of the thoracic rings while the musculature associated with the lost components was retained. The alternative hypothesis, given by Manton (1961), was that the thoracic rings acquired new muscles similar to those that normally occur on the posterior pair of legs or sternite of a diplosegment.

After a survey of chilognath diplopod skeletomuscular anatomy, Demange (1967) concluded that the thorax, inclusive of the collum, is composed of four diplosegments each with a single pair of legs. This conclusion was based on several lines of skeletomuscular evidence: the muscular complexity of the thoracic rings, the presence of intercalary sclerites, and the presence of paired genitalia. In Demange's scenario, the thoracic legs represent the anterior pair of a diplosegment, the posterior pair having been suppressed. Demange interpreted the presence of the intercalary sclerites posterior to the appendages on the thoracic rings and their associated musculature as remnants of the posterior appendage pair. This interpretation was contrary to that of Brölemann (1920), who favored the hypothesis that the intercalary sclerites represented evolutionary novelties and not highly atrophied appendages. Following along the same lines, Demange (1967) also interpreted the penes of the male and the cyphopods of the female as appendage derivatives, thus providing evidence for the diplosomitic nature of the second postcollum ring. Demange (1967) hypothesized that the penes and cyphopods were free in basal millipede taxa and in more derived groups, the genital organs became fused to the appendages, and discernable intercalary sclerites were lost.

There are several difficulties with Demange's (1967) conclusions regarding the segmental implications of the penes, cyphopods, and intercalary sclerites. The first is phylogenetic, as it is apparent that they were formulated in the context of a phylogenetic scheme in which juliform millipedes were basal to the Colobognatha (= Platydesmida + Siphonophorida + Polyzoniida). This phylogeny is the inverse of that produced by recent phylogenetic analyses in which juliform millipedes have consistently been found to be the most derived (e.g., Enghoff, 1984; Enghoff et al., 1993). In male millipedes the gonopores either open on the coxae of the second pair of legs (or through penes on them) (Pentazonia, some Colobognatha, Chordeumatida, and Polydesmida) or on paired or unpaired penes posterior to the second pair of legs (Penicillata, Stem-

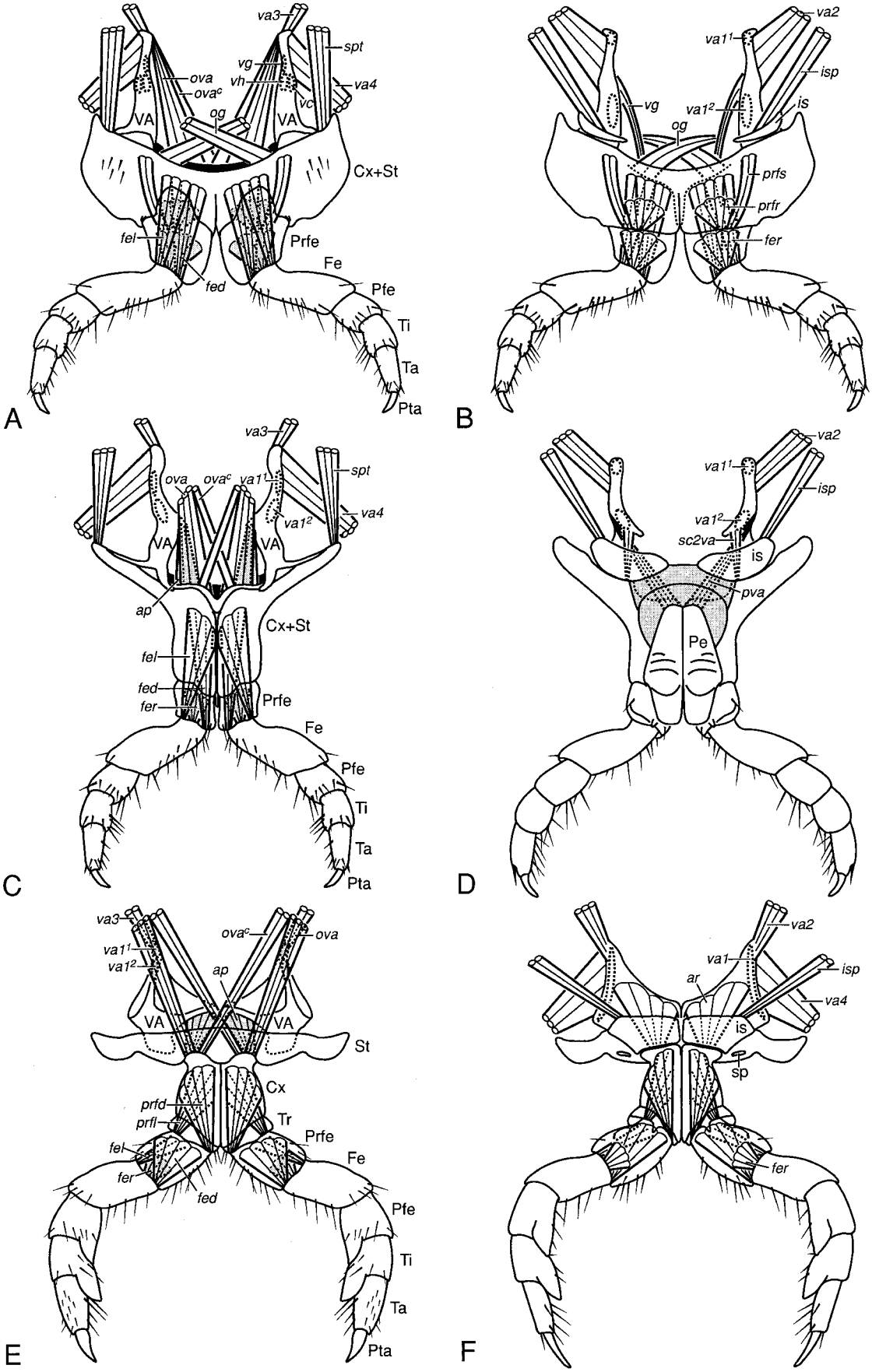
A
va3
spt
vg
ova
vh
va4
ovac
vc
og
VA
VA
Cx+St
fel
Prfe
Fe
fed
Pfe
Ti
Ta
Pta
B
va2
va11
isp
vg
va12
is
og
prfs
prfr
fer
C
va3
spt
ova
ovac
va11
va4
va12
VA
VA
ap
Cx+St
fel
fed
fer
Prfe
Fe
Pfe
Ti
Ta
Pta
D
va2
va11
isp
va12
sc2va
is
pva
Pe
E
va3
ovac
ova
va11
va12
ap
VA
VA
St
Cx
prfd
prfl
Tr
Prfe
fel
Fe
fer
fed
Pfe
Ti
Ta
Pta
F
va2
va1
isp
ar
va4
is
sp
fer

Figure 10

miulida, Juliformia, and some Colobognatha) (Enghoff, 1990). Thus, the presence of free penes posterior to the second leg pair is likely a derived character (Enghoff, 1990). In addition, intercalary sclerites are only found in the Juliformia and are not present in more basal taxa. The second difficulty with Demange's (1967) conclusions is a matter of counting. Intercalary sclerites are found posterior to leg pairs 1–3 in *Phyllogonostreptus* and the penes are located posterior to leg pair 2. If both the intercalary sclerites and penes actually represented modified appendages, then thoracic ring 2 would be a triplosegment. Demange skirts this difficulty by suggesting that the intercalary sclerite posterior to the second leg and the genital organ were derived from the same appendage without giving any convincing morphological justification for this relationship. However, there is nothing in the morphology of *Phyllogonostreptus* to suggest that the penes and intercalary sclerites of the second thoracic ring are ontogenetically related structures.

Skeletomuscular evidence aside, soft-tissue evidence strongly points toward thoracic rings each being representative of a single somite. Each thoracic ring has only one ganglion (Miley, 1930) and only one pair each of ostia, lateral heart arteries, and alary muscles (Seifert, 1932). Each of the undisputed diplosegments has two ganglia (Miley, 1930) and two pairs each of ostia, lateral arteries, and alary muscles (Seifert, 1932). However, this evidence does not seem to be enough to convince the skeptics, as there is a recurring sentiment in the literature that the morphological state of the adult is not necessarily a good indicator of underlying homology. For example, Manton (1954) suggested that it would not be surprising to find a correlation between the loss of appendages in a diplosegment and the loss of an external distinction between two pairs of ganglionic rudiments in the embryo. Along the same lines, Kraus (1990) cited the appearance of two tergal and pleural sclerites on trunk rings 2, 3, and 4 in some premolt polydesmids as evidence for the diplosomitic identity of these rings. However, Enghoff et al. (1993) were unconvinced as to the significance of this thoracic tergal and pleural disintegration in light of the concurrent pattern of premolt sternal disintegration on midbody rings. They pointed out that each midbody ring disintegrates into an anterior apodous ventral sclerite and a posterior sclerite with two pairs of legs. These two sclerites clearly do not correspond to the original sterna.

The current embryological evidence does not support the diplosomitic nature of the thoracic rings. Dohle (1964, 1974) was able to correlate embryonic leg-bearing somites with the tergite (t), or portion thereof, that they produced. He found that the first leg-bearing embryonic somite forms the posterior portion of the collum (t1), the second leg-bearing embryonic somite forms the posterior portion of t2, the third embryonic leg-bearing somite forms t3, the fourth embryonic leg-bearing somite forms t4, and the fifth plus the sixth embryonic leg-bearing somites form t5, the first diplotergite. Dohle (1964, 1974) never observed anything in the development of millipede embryos to suggest that a second pair of appendages was phylogenetically suppressed in the thoracic rings.

The argument that thoracic rings are modified diplosegments seems difficult to accept, given anatomical and developmental evidence pointing to their monosomitic composition. Thus, an alternative explanation needs to be sought for the muscular complexity of the thoracic rings. In her consideration of the difference in musculature between the thorax and postthoracic rings, Manton (1961) did not consider a third, more parsimonious hypothesis put forward here: that the thoracic rings did not double-up on muscles or gain new muscles, but that the postthoracic rings have lost muscles relative to the thoracic rings.

Millipedes belonging to the basal orders Polyxenida, Glomeridesmida, Glomerida, Sphaerotheriida, and Polyzoniida have free sternites, tergites, and pleurites. Correspondingly, they have more complex trunk musculature than ring-forming millipedes. In addition, the trunk musculature in these basal groups exhibits very little anterior–posterior variation. Following upon this, it seems reasonable to hypothesize that juliform millipedes retain an ancestral level of muscular complexity in the thoracic rings, which retain free sternites, and that the postthoracic rings have undergone a loss of musculature correlated with the fusion of sternites, pleurites, and tergites into complete rings.

The hypothesis stated above can be tested by looking at another group of ring-forming millipedes, the Polydesmida. As in the Juliformia, the first three postcollum rings have only one pair of legs each. However, in the Polydesmida only the sternites of the first and second postcollum rings are free: the sternites of the third postcollum ring and those of the remainder of the trunk are incorporated into seamless body rings. As predicted, the musculature of the third postcollum ring is comparable to the posterior trunk rings, while the musculature of the first and second postcollum rings is relatively more complex (Manton, 1961, text, fig. 24; Demange, 1967, fig. 16).

When the available anatomical evidence is considered within a phylogenetic context, it seems likely

Fig. 10. *Phyllogonostreptus nigrolabiatus*. Skeletomuscular anatomy of the first three pairs of legs. **A**: Anterior view of first leg pair. **B**: Posterior view of first leg pair. **C**: Anterior view of second leg pair. **D:** Posterior view of second leg pair. **E**: Anterior view of third leg pair. **F**: Posterior view of third leg pair. Muscle abbreviations are defined in Table 1. Cx, coxa; Fe, femur; is, intercalary sclerite; Pe, penis; Pfe, postfemur; Prfe, prefemur; Pta, posttarsus; sp, spiracle; St, sternite; Ta, tarsus; Ti, tibia; Tr, trochanter; VA, ventral apodeme.

TABLE 2. Homologous cephalic muscles in the julid Cylindroiulus teutonicus *(Pocock) (=* C. caeruleocinctus *(Wood)) and the spirostreptid* Phyllogonostreptus nigrolabiatus *Newport**

Phyllogonostreptus nigrolabiatus		*Cylindroiulus teutonicus*	
No.	Name	No.	Name
a1	Median septum antennal m.	28	M. phragmo vertico-scapalis posterior
a2	Medial antennal m.	26	M. tentorio-scapalis medius
a3	Lateral antennal m.	25	M. tentorio-scapalis lateralis
a4	Anterior antennal m.	27	M. tentorio-scapalis anterior
e1	Anterior epipharyngeal m.	16	M. clypeo-epipharyngalis lateralis
e2	Posterior epipharyngeal m.	17	M. frontoclypeo-epipharyngalis medialis
e3	Posterolateral epipharyngeal m.	15	M. frontoclypeo-epipharyngalis anterior
e4	Anterolateral epipharyngeal m.	—	no homolog
g1	Lingual lobe m.	10	M. suspensorio-lamella lingualis
g2	Anterior gnathochilarial stipes m.	9	M. suspensorio-stipitalis
g3	Lateral mentum m.	—	no homolog
g4	Anteromedial mentum m.	13	M. endochilario-stipitalis
g5	Posteromedial mentum m.	—	no homolog
g6	Posterolateral gnathochilarial stipes m.	12	M. phragmo occipito-stipitalis
g7	Posteromedial gnathochilarial stipes m.	11	M. ligamento intergnathaleo-stipitalis
g8	Medial intermentum m.	—	no homolog
g9	Lateral intermentum m.	—	no homolog
m1	Gnathal lobe sclerite m.	7	M. phragmo vertico-tendo mandibularis
m2	Dorsal mandibular stipes m.	6	M. phragmo-occipitalis mandibula distalis
m3	Proximal gnathal lobe m.	—	no homolog
m4	Anterior mandibular cardo m.	4	M. tentorio-mandibula proximalis
m5	Posterior mandibular stipes m.	3	M. tentorio-mandibula distalis
m6	Ventral mandibular stipes m.	1	M. ligamento intergnathaleo-mandibula distalis
m7	Anterior mandibular stipes m.	—	no homolog
m8	Gnathal lobe m.	8	M. ligamento intergnathaleo-mandibula gnathalis
m9	Posterior mandibular cardo m.	2	M. ligamento intergnathaleo-mandibula proximalis
p1	Precerebral pharyngeal dilator m.	18	M. frontoclypeo-epipharyngalis posterior
p2	Intercerebral pharyngeal dilator m.	19	M. fronto-pharyngalis anterior
p3	Median septum pharyngeal dilator m.	20	M. phragmo vertico-pharyngalis
p4	Dorsal postoccipital flange pharyngeal dilator m.	22	M. phragmo occipito-pharyngalis lateralis posterior
p5	Tentorial pharyngeal dilator m.	21	M. tentorio-pharyngalis lateralis anterior
p6	Transverse mandibular tendon pharyngeal dilator m.	23	M. ligamento intergnathaleo-pharyngalis ventralis anterior
p7	Ventral postoccipital flange pharyngeal dilator m.	24	M. präbasilaro-pharyngalis ventralis posterior
t1	Anterior tentorial m.	14	M. clypeo-tentorialis
t2	Dorsal tentorial m.	—	no homolog
t3	Posterior tentorial m.	5	M. tentorio-phragmo occipitalis

*The numbers and names given to the muscles in *C. teutonicus* are those of Fechter (1961).

that the skeletomuscular anatomy of the postthoracic rings of ring-forming millipedes is more derived than that of the thoracic rings. This represents the opposite of the case required by proponents of the thoracic diplosegment hypothesis, in which the skeletomuscular anatomy of the thoracic rings is derived relative to the postthoracic rings. Thus, combining the muscular evidence with that of the embryological development, nervous, and circulatory systems, it seems very difficult to make a case for the diplosomotic nature of the millipede thoracic rings.

ACKNOWLEDGMENTS

I thank Jeffrey Shultz for financial support, the use of laboratory facilities, and comments on the manuscript, and Richard Hoffman for identifying *Phyllogonostreptus nigrolabiatus* and providing information on juliform gonopods. I also thank two anonymous reviewers for helpful comments.

LITERATURE CITED

Bodine MW. 1970. The segmental origin of the appendages of the head and anterior body segments of a spiroboloid milliped, *Narceus annularis*. J Morphol 132:47–68.

Brölemann HW. 1916. Les gonopodes des Spirostreptes (Myriap. Diplop.). Note préliminaire. Bull Soc Ent France 21:51–53.

Brölemann HW. 1920. Voyage de Ch. Alluaud et R. Jeannel en Afrique Orientale (1911–1912). Résultats Scientifiques. Myriapodes III, Diplopoda. Paris: Librarie des Sciences naturelles Léon L'homme.

Brölemann HW. 1935. Myriapodes Diplopodes (Chilognathes I). Faune de France 29. Paris: Paul Lechevalier.

Demange J-M. 1964. Les appendices postérieurs (9^{e} paire) du diplosegment gonopodial (VII^{e}) des Spirostreptoidea (Myriapodes Diplopodes). Bull Mus Nat Hist Nat 2^{e} ser 36:191–210.

Demange J-M. 1967. Recherches sur la segmentation du tronc des Chilopodes et des Diplopodes Chilognathes (Myriapodes). Mém Mus Nat Hist Nat (A) 44:1–188.

Dohle W. 1964. Die Embryonalentwicklung von *Glomeris marginata* (Villers) im Vergleich zur Entwicklung anderer Diplopoden. Zool Jb (Anat) 81:241–310.

Dohle W. 1974. The segmentation of the germ band of Diplopoda compared with other classes of arthropods. In: Blower JG, editor. Myriapoda. Symp Zool Soc Lond 32. London: Academic Press. p 143–161.

Enghoff H. 1981. A cladistic analysis and classification of the millipede order Julida. Z Zool Syst Evolut-forsch 19:285–319.

Enghoff H. 1984.Phylogeny of millipedes—a cladistic analysis. Z Zool Syst Evolut-forsch 22:8–26.

Enghoff H. 1990. The ground-plan of chilognathan millipedes (external morphology). In: Minelli A, editor. Proc 7th Int Congress Myriapodology. Leiden: E.J. Brill. p 1–21.

Enghoff H. 1991. A revised cladistic analysis and classification of the millipede order Julida. Z Zool Syst Evolut-forsch 29:241–263.

Enghoff H. 1995. A revision of the Paectophyllini and Calyptophyllini: millipedes of the Middle East (Diplopoda: Julida: Julidae). J Nat Hist 29:685–786.

Enghoff H, Dohle W, Blower JG. 1993. Anamorphosis in millipedes (Diplopoda)—the present state of knowledge with some developmental and phylogenetic considerations. Zool J Linnean Soc 109:103–234.

Fechter H. 1961. Anatomie und Funktion der Kopfmuskulatur von *Cylindroiulus teutonicus* (Pocock). Zool Jb Anat 79:479–528.

Hoffman RL. 1982. Diplopoda. In: Parker SP, editor. Synopsis and classification of living organisms. New York: McGraw-Hill. p 689–724.

Hoffman RL, Orcutt BS. 1960. A synopsis of the Atopetholidae, a family of spiroboloid millipeds. Proc US Nat Mus 111:95–166.

Jeekel CAW. 1985. The distribution of the Diplocheta and the "lost" continent of Pacifica (Diplopoda). Bijdr Dierk 55:100–112.

Kraus O. 1990. On the so-called thoracic segments in Diplopoda. In: Minelli A, editor. Proc 7th Int Congress Myriapodology. Leiden: E.J. Brill. p 63–68.

Latzel R. 1884. Die Myriopoden der österreichisch-ungarischen Monarchie. 2 Hälfte. Wien: Alfred Hölder.

Manton SM. 1954. The evolution of arthropodan locomotory mechanisms. 4. The structure, habits and evolution of the Diplopoda. J Linn Soc (Zool) 42:299–368.

Manton SM 1956. The evolution of arthropodan locomotory mechanisms. 5. The structure, habits and evolution of the Pselaphognatha (Diplopoda). J Linn Soc (Zool) 43:153–187.

Manton SM. 1958. The evolution of arthropodan locomotory mechanisms. 6. Habits and evolution of the Lysiopetaloidea (Diplopoda), some principles of leg design in Diplopoda and Chilopoda, and limb structure in Diplopoda. J Linn Soc (Zool) 43:487–556.

Manton SM. 1961. The evolution of arthropodan evolutionary mechanisms. 7. Functional requirements and body design in Colobognatha (Diplopoda), together with a comparative account of diplopod burrowing techniques, trunk musculature and segmentation. J Linn Soc (Zool) 44:383–461.

Manton SM. 1964.Mandibular mechanisms and the evolution of arthropods. Philos Trans R Soc London B247:1–183.

Miley HH. 1930. Internal anatomy of *Euryurus erythropygus* (Brandt). (Diplopoda). Ohio J Sci 30:229–255.

Pflugfelder O. 1932. Über den Mechanismus der Segmentbildung bei der Embryonalentwicklung und Anamorphose von *Platyrracus amauros* Attems. Z Wiss Zool 140:650–723.

Regier JC, Shultz JW. In press. phylogenetic analysis of Myriapoda (Arthropoda) using two nuclear protein-encoding genes. Zool J Linn Soc.

Shultz JW. 1993. Muscular anatomy of the giant whipscorpion *Mastigoproctus giganteus* (Arachnida, Uropygi), and its evolutionary significance. Zool J Linn Soc 108:335–365.

Shultz JW. 1999. Muscular anatomy of a whipspider, *Phrynus longipes* (Pocock) (Arachnida: Amblypygi), and its evolutionary significance. Zool J Linn Soc 126:81–116.

Shultz JW. 2000. Skeletomuscular anatomy of the harvestman *Leiobunum aldrichi* (Weed, 1893) (Arachnida: Opiliones) and its evolutionary significance. Zool J Linn Soc 128:401–438.

Seifert B. 1932. Anatomie und Biologie des Diplopoden *Strongylosoma pallipes* Oliv. Z Morph Ökol Tiere 25:362–507.

Silvestri P. 1903. Classis Diplopoda, vol. 1, Anatome. Portici.

Verhoeff KW. 1911. Zur Kenntnis des Mentum der Iuloidea und über Protoiuliden. Zool Anz 38:531–546.

Verhoeff KW. 1926–1932. Klasse Diplopoda. In: Bronn HG, editor. Klassen und Ordnungen des Tier-Reichs, vol. 5. Book 2. Leipzig: Akademische Verlagsgesellschaft m.b.H.